



HAL
open science

Automation of quality control and reduction of non-compliance using machine learning techniques at Faurecia Clean Mobility

Charbel El Hachem

► **To cite this version:**

Charbel El Hachem. Automation of quality control and reduction of non-compliance using machine learning techniques at Faurecia Clean Mobility. Artificial Intelligence [cs.AI]. Université Bourgogne Franche-Comté, 2022. English. NNT : 2022UBFCD011 . tel-03775370

HAL Id: tel-03775370

<https://theses.hal.science/tel-03775370>

Submitted on 12 Sep 2022

HAL is a multi-disciplinary open access archive for the deposit and dissemination of scientific research documents, whether they are published or not. The documents may come from teaching and research institutions in France or abroad, or from public or private research centers.

L'archive ouverte pluridisciplinaire **HAL**, est destinée au dépôt et à la diffusion de documents scientifiques de niveau recherche, publiés ou non, émanant des établissements d'enseignement et de recherche français ou étrangers, des laboratoires publics ou privés.

THÈSE DE DOCTORAT
DE L'ÉTABLISSEMENT UNIVERSITÉ BOURGOGNE FRANCHE-COMTÉ
PRÉPARÉE À L'UNIVERSITÉ DE FRANCHE-COMTÉ

École doctorale n°37
Sciences Pour l'Ingénieur et Microtechniques

Doctorat d'Informatique

par

CHARBEL EL HACHEM

**Automation of Quality Control and Reduction of Non-Compliance using
Machine Learning Techniques at Faurecia Clean Mobility**

**Automatisation du contrôle qualité et réduction des non conformités en utilisant des
techniques de machine learning chez Faurecia Clean Mobility**

Thèse présentée et soutenue à Belfort, le 14 Avril 2022

Composition du Jury :

PROF CHRÉTIEN STÉPHANE	Université de Lyon 2	Rapporteur
DR VERNIER FLAVIEN	Université Savoie Mont Blanc	Rapporteur
PROF CONTASSOT-VIVIER SYLVAIN	Université de Lorraine	Examineur
PROF COUTURIER RAPHAËL	Université Bourgogne Franche-Comté	Directeur de thèse
DR PERROT GILLES	Université Bourgogne Franche-Comté	Codirecteur de thèse
M. PAINVIN Loïc	Faurecia Clean Mobility	Encadrant en entreprise

ABSTRACT

Automation of Quality Control and Reduction of Non-Compliance using Machine Learning Techniques at Faurecia Clean Mobility

Charbel El Hachem
University of Bourgogne Franche Comté, 2022

Supervisors: Raphaël Couturier, Gilles Perrot and Loïc Painvin

Quality control applications in the automotive industry are numerous. Automotive companies are working on the automation of these applications and add a particular focus on securing their processes.

In this thesis, the first contribution proposes an automated quality control for component presence. It allows to classify if the component is present, missing or has been replaced by another component. The algorithm can achieve an accuracy of 100% with live tests.

The second contribution focuses on automating the quality control of welding seams that haven't been reached by leak tests, covering external aspects of welding defects. The images collected from the plants are not balanced, data augmentation techniques have been applied to reach more balanced dataset. In this contribution, a standard deep learning algorithm applied on raw data has been compared to data augmentation approaches. The target, defined by the plant, 97% of defected reference parts detection, has been reached on half of the welds. The challenge remains present on the other half.

In the third contribution, deep learning model explainability and welding seams classification accuracy are combined. A hybrid approach of CNN-Machine learning classifier is proposed to improve the accuracy reached in the second contribution. This work presents a new model-driven optimization reaching an accuracy above 98% when applied on welding seams dataset.

In the fourth contribution, ceramic monolith position and their relative breakages are studied. The quality control of these monoliths should be done during the production of exhaust pipes. A comparison between image processing filters for straight lines detection is presented. The tests were carried out by applying a rotation to the ceramic in a 5-degree step. The results show that canny filter applied with hough lines allows to achieve an

accuracy of 99%.

Finally, a Human Machine Interface (HMI) has been developed aiming to provide a Plug & Play system to the plants. The integration of this digital solution in the plant's cycle time will be discussed, as well as its architecture.

KEYWORDS: deep learning, image classification, convolutional neural network, data augmentation, industry automation

RÉSUMÉ

Automatisation du contrôle qualité et réduction des non conformités en utilisant des techniques de machine learning chez Faurecia Clean Mobility

Charbel El Hachem
Université de Bourgogne Franche Comté, 2022

Encadrants: Raphaël Couturier, Gilles Perrot and Loïc Painvin

Les applications de contrôle qualité dans l'industrie automobile sont nombreuses. Les constructeurs automobiles travaillent sur l'automatisation de ces applications et mettent un accent particulier sur la sécurité de leurs processus. Dans cette thèse, la première contribution propose un contrôle automatisé de présence de composants. La méthode proposée permet de déterminer si le composant est présent, absent ou a été remplacé par un autre composant. L'algorithme peut atteindre une précision de 100% avec des tests en conditions réelles.

La deuxième contribution porte sur la classification des cordons de soudure non atteints par les tests d'étanchéité. Cette classification est relative aux aspects externes des soudures. Les images collectées à partir des usines ne sont pas équitablement réparties sur les classes du modèle d'intelligence artificielle. Des techniques d'augmentation de données ont été appliquées pour atteindre un ensemble de données mieux réparti. Dans cette contribution, un algorithme standard d'apprentissage profond appliqué sur des données brutes a été comparé à des approches d'augmentation de données. L'objectif, défini par l'usine, de 97% de détection des pièces de référence défectueuses a été atteint sur deux soudures. Le défi reste présent sur les deux autres soudures.

Dans la troisième contribution, une approche hybride de CNN-Machine Learning Classifier est proposée pour améliorer la précision atteinte dans la seconde contribution. Ce travail présente une nouvelle optimisation pilotée par un modèle atteignant une précision supérieure à 98% lorsqu'elle est appliquée sur un jeu de données de cordons de soudure. Dans la quatrième contribution, les criques de monolithes en céramique sont étudiées. Leur contrôle qualité doit se faire lors de la fabrication de pots d'échappement. Une

comparaison entre différents filtres de traitement d'images permettant la détection de l'orientation de la céramique est présentée. Les tests ont été réalisés en appliquant une rotation de la céramique par pas de 5 degrés. Les résultats montrent qu'avec la méthode *canny + hough lines*, une précision de 99% est atteinte.

Enfin, une Interface Homme Machine (IHM) a été développée et son objectif est de fournir un système Plug & Play aux usines. Cette contribution abordera les étapes à suivre pour déployer une solution numérique : son intégration dans le temps de cycle de l'usine suivant le Système de Gestion du Programme d'Innovation et son architecture.

Mots clés: apprentissage profond, classification d'images, réseau neuronal convolutif, augmentation de données, automatisation de l'industrie

ACKNOWLEDGEMENTS

I would like to thank the following people, without whom I would not have been able to complete this research, and without whom I would not have made it through my Ph.D degree:

My supervisor Dr. Raphaël COUTURIER, for his enthusiasm for the project, for his support, encouragement, and patience. The meetings and conversations were vital in inspiring me to think outside the box, from multiple perspectives to form a comprehensive and objective critique.

My Faurecia manager Mr. Loïc PAINVIN who guided me so positively and who always made me feel confident in my abilities. Thank you for being a manager who cares so much about his employees and for all the opportunities you have given me to advance my career.

I would like to thank my thesis co-supervisor Dr. Gilles PERROT, whose support and remarks allowed my studies to go the extra mile.

I am forever thankful to my colleagues at Faurecia for their friendship and support, and for creating a cordial working environment. Thank you for making the work environment memorable.

I would also like to thank the pedagogical and administrative team at University Institute of Technology at Belfort and anyone who has contributed near or far to the realization of this work.

Special thanks goes to Mr. Laurent BILLAUD, Mr. Frédéric BLANCO and Dr. Youssef BOU ISSA, for their trust and support.

Finally, my deep and sincere gratitude to my family for their continuous and exceptional love, help and support. I am grateful to my sisters Patricia, Nadine, Najoie and Pamela for always being there for me. I would also like to thank my nieces and nephews, Laeticia, Joseph, Georgio, Elçin and Brandon, who were my source of motivation.

I am forever indebted to my parents for giving me the opportunities and experiences that have made me who I am. They selflessly devoted their lives to their children and here I am dedicating this milestone to them. I love you mom and dad.

CONTENTS

I	Dissertation introduction	3
1	Introduction	5
1.1	Thesis context	5
1.2	Introduction to industry automation	6
1.3	Use case: quality control in the automotive industry	7
1.4	Main contributions of this dissertation	7
1.5	Dissertation outline	8
II	Industrial context: quality control in the automotive industry	11
2	Types of quality control in the automotive industry	13
2.1	Introduction	13
2.2	Product life cycle in Faurecia plants	13
2.3	Industry automation	13
2.4	Existing solutions in the market	14
2.4.1	Examples of quality control	14
2.5	Conclusion	16
3	Neural network based computer vision	17
3.1	Introduction	17
3.2	Computer vision definition	17
3.3	Artificial intelligence definition	18
3.4	Machine learning	18
3.4.1	Machine learning systems	19
3.4.2	Types of learning	19

3.4.3	Challenges of machine learning	19
3.4.4	Confusion matrix	20
3.5	Deep learning	21
3.5.1	Convolutional neural network	22
3.5.2	Convolutional neural network applications	22
3.5.3	How convolutional neural networks work	22
3.5.4	Steps to design a neural network	26
3.6	CNN architectures	26
3.6.1	ResNet50 applications	27
3.6.2	ResNet50 architecture	27
3.6.3	MobileNet applications	29
3.6.4	MobileNet architecture	29
3.7	Image processing	29
3.8	Conclusion	30
III	Contributions	31
4	Component Presence Control	33
4.1	Introduction	33
4.2	Problem statement	34
4.3	Automatic control implementation	35
4.3.1	Data collection	35
4.3.2	Analysis of the collected data	35
4.3.3	Experimental environment	36
4.4	Experimental results	36
4.4.1	Accuracy improvements	36
4.4.2	Cycle time and reliability improvements	37
4.5	Conclusion	38
5	Welding Seam Classification	41
5.1	Introduction	41

5.2	Welding seams in the automotive industry	42
5.2.1	Types of weld joints	42
5.2.2	Types of welding technologies	44
5.2.3	Types of welding seams quality control	44
5.2.4	Welding seams inspection	46
5.2.5	Leak test	47
5.3	Visual inspection of welding seams in Faurecia plants	48
5.3.1	Reference part	48
5.3.2	Data collection	48
5.3.3	Operating procedure	50
5.3.4	Parameters contributing to the quality of welding seams	50
5.4	Deep learning solution for automated welding seams quality control	50
5.4.1	Dataset challenges	51
5.4.2	Data augmentation definition	51
5.4.3	Data augmentation filters	52
5.5	Implementation details	53
5.5.1	Analysis of the collected data	53
5.5.2	Cross validation	53
5.5.3	Experimental environment	55
5.6	Experimental results	55
5.7	Conclusion	56
6	AI parameters correlation	57
6.1	Introduction	57
6.2	Parameters correlation	58
6.2.1	Visual explanation of the heatmap	58
6.2.2	Deep learning accuracy calculation	58
6.2.3	Model reliability	59
6.3	State of the art of hybrid methods	60
6.4	Methods for improving the AI model reliability	61

6.4.1	Model explainability	61
6.4.2	Heatmap analysis	61
6.4.3	Machine learning classifiers	62
6.5	Implementation details	64
6.5.1	Data collection	64
6.5.2	Experimental environment	65
6.6	Experimental results	65
6.7	Conclusion	65
7	Brick orientation adjustment	67
7.1	Introduction	67
7.2	Problem statement	68
7.2.1	Stuffing technique	68
7.2.2	Risk of breakage	69
7.2.3	Deep learning vs. image processing	69
7.2.4	Angle analysis	69
7.3	Image processing methods for angular position measurement	70
7.3.1	Highlighting edges	70
7.3.2	Hough lines	71
7.4	Implementation details	71
7.4.1	Experimental Environment	71
7.4.2	Images collection	72
7.4.3	Vision parameters	72
7.5	Experimental results	74
7.5.1	Coefficient of determination	74
7.5.2	Repeatability test	75
7.6	Conclusion	75
8	Towards autonomous plants	77
8.1	Introduction	77
8.2	Problem statement	77

8.2.1	Features required in plants	77
8.2.2	Network architecture	78
8.2.3	Cycle time of a turntable	78
8.3	Software development context	78
8.3.1	Agile methodology	79
8.3.2	HMI development	81
8.3.3	HMI architecture	85
8.4	Industrial context	85
8.4.1	Innovation Program Management System (IPMS) steps	85
8.4.2	Release phases	86
8.5	Added value of the proposed solution	87
8.6	Conclusion	87
IV	Conclusion & perspectives	89
9	Conclusion & perspectives	91
9.1	Conclusion	91
9.2	Perspectives	92

LIST OF ABBREVIATIONS

DE&D	Digital Expertise and Development
R&D	Research and Development
FCM	Faurecia Clean Mobility
CNC	Computer Numerical Controls
AI	Artificial Intelligence
POC	Proof of Concept
HMI	Human Machine Interface
CAD	Computer-Aided Design
OEE	Overall Equipment Effectiveness
CNN	Convolutional Neural Network
SVM	Support Vector Machine
IPMS	Innovation Program Management System
GAN	Generative Adversarial Network
YOLO	You Only Look Once
VGG	Visual Geometry Group
ResNet	Residual Network
RN	Recurrent Networks
RGB	Red Green Blue
NOK	NOT OK
ReLU	Rectified Linear Unit
SE	Squeeze-and-Excitation
CPU	Central Processing Unit
MAG	Metal Active Gas
TIG	Tungsten Inert Gas
PAW	Plasma Arc Welding
MF1	Main Function

MIG	Metal Inert Gas
PLC	Programmable Logic Controller
PC	Personal Computer
RMSProp	Root Mean Squared Propagation
Grad-CAM	Gradient-weighted Class Activation Mapping
MNIST	Modified National Institute of Standards and Technology
LSTM	Long Short-Term Memory
RCR	Red Color Ratio
KNN	K-Nearest Neighbor
XG-Boost	Extreme Gradient Boosting
RAM	Random-Access Memory
UML	Unified Modeling Language
Ph.D	Doctor of Philosophy
MPT	Mass Production Trial
CRUD	Create Read Update Delete



DISSERTATION INTRODUCTION

INTRODUCTION

This thesis focuses on advancing the state-of-the-art of quality control in the automotive industry, with a specific focus on component presence control, welding seam classification, and brick orientation adjustment. The presented research was carried out in a CIFRE thesis: a collaboration between Faurecia Clean Mobility and the Department of Informatics and Complex Systems (DISC in French) of FEMTO-ST Institute laboratory. Throughout the remainder of this thesis, the writer will be referred to as “we”, rather than “I”. This is because this thesis presents research performed in a collaborative setting in Bavans-France, as part of the Digital Expertise and Development (DE&D) innovation laboratory team.

This chapter provides an introduction to the work conducted in this thesis. It addresses the general context and the considered quality control use cases, then presents briefly the contributions of this thesis.

1.1/ THESIS CONTEXT

This thesis is an industry oriented research, aiming to apply academic research results for manufacturing profit by using research to improve industrial processes. Faurecia is a major actor in the Automotive industry and develops technologies for sustainable mobility and personalized experiences for the Cockpit of the Future.

This thesis is mainly located at the Research and Development (R&D) center of Faurecia Clean Mobility, more specifically in the DE&D service. This business group is exhaust systems oriented: vast number of references is produced and copies of the same reference may have dissimilarities. For that, quality control is necessary and should be applied to every reference part.

1.2/ INTRODUCTION TO INDUSTRY AUTOMATION

By definition, quality control is testing an output sample against specifications. In the manufacturing sector, the plant follows the specification needs to respond to the client's requirement before delivering products. Quality control applications in the automotive industry are numerous, and today's manufacturing industry has enabled the use of artificial intelligence and image processing algorithms in its applications. These applications allow the automation of quality control making by that the plants autonomous. A great deal of work has been done recently with deep learning and image processing in the manufacturing sector, and the benefits on the production line are significant. One evolving role of artificial intelligence is to be able to learn continuously and to progress by time. Automated quality control in the production line will allow the reduction of unnecessary tasks, shocking the cycle time. Earnings of this automation are calculated in terms of maintaining the continuity of the process.

Factory automation is the incorporation of automation from end-to-end manufacturing processes. Industrial automation uses control systems and equipment, whether computers, process controllers or robots to replace a human being. Automation increases productivity, eliminates error, and allows for better control of the manufacturing process. Three types of industry automation systems can be identified: the first one is the fixed system, where the production equipment is fixed and is often used to execute repetitive tasks. Assembly lines in the automotive industry are an example of fixed systems. The second one is the programmable system, used in batch process production. It is able to be reconfigured depending on the batches of products and their specifications. Industrial robots are an example of programmable system. The third one is the flexible automation system, used when the product changes frequently. Each particular job requires a code, the necessary tools and equipment for the production. The product changeovers are brought by the control system, no time needed for reconfiguration between batches. Computer Numerical Controls (CNC) machines are an example of flexible system. Artificial intelligence (AI) and image processing techniques has become indispensable in the industry automation, particularly in quality control systems.

The work done in this thesis addresses numerous algorithms ready to be deployed in a manufacturing environment. All of the developed solutions follow an industrial process so they can be deployed: starting with a proof of concept (POC), a prototype, a pilote and finally a standardized solution is obtained. The data studied in this work correspond to 2D images collected from Faurecia plants. The purpose of this thesis is therefore to suggest digital solutions to automotive plants. The contributions concentrate specifically on component presence control, welding seam classification and brick orientation adjustment in which various deep learning and image processing approaches are presented to solve different challenges. Lastly, the final contribution is relative to the Human Machine

Interface (HMI) that has been developed to provide the plants with a Plug & Play system.

1.3/ USE CASE: QUALITY CONTROL IN THE AUTOMOTIVE INDUSTRY

Different types of quality control are done in the automotive industry, such as component presence control, welding seam classification, geometric control, and brick orientation adjustment. Two main parameters should be taken into consideration when automating quality control. Firstly, is the integration in the production line; proof of concept realized at the innovation laboratory has different environment conditions compared to plants. Secondly, the impact on the cycle time has to be taken into consideration so the production won't be affected by the algorithm execution time.

1.4/ MAIN CONTRIBUTIONS OF THIS DISSERTATION

The main contributions in this dissertation fall within the automation of quality control by applying artificial intelligence and image processing techniques to classify extracted features. The main contributions can be summarized as follows:

1. We proposed an automated quality control for component presence. The proposed method is based on ResNet50 architecture and allows to classify if the component is present, missing or replaced by another component. This algorithm is able to achieve an accuracy of 99% with live tests. Furthermore, the other performance matrices used in this work are reliability and cycle time. A comparison between the software execution time and human inspection is presented. The results show that automating component presence control obtains better Overall Equipment Effectiveness (OEE) than manual inspection and avoids performance degradation over the operator's shift.
2. Classification of welding seams is performed using a deep neural network. Four welding seams are not covered by leak tests, this is why visual inspection is necessary. This classification is relative to external aspects of welding defects. The images collected from the plants are imbalanced between classes, data augmentation techniques have been applied to reach more balanced dataset. MobileNet architecture has been used for image classification. In this contribution, a standard deep learning algorithm applied on raw data has been compared to data augmentation approaches. The target, defined by the plant's team, of 97% of detection of

defected reference parts has been reached on two welds. The challenge remains present on two other welds.

3. We emphasize the contribution of deep learning model explainability and the improvement of welding seams classification accuracy obtained in the second contribution. A hybrid approach of CNN-Machine Learning Classifier is proposed, combining the model prediction scores and visual explanation heatmap. The hybrid approach proposed in this paper reaches high accuracy on weld defects classification. The highest accuracy improvement was by +72.7% for the second weld using MobileNet-XGboost classifier and by +22.6% for the third weld using MobileNet-SVM Poly5 Kernel or MobileNet-XGboost classifier.
4. Ceramic monoliths risk breakage during production. This is due to their position at a specific angle. Quality control should be done on each brick during the production of the exhaust pipes. This control aims to adjust, if needed, the positioning of the brick before starting the production. We compared several image processing filters for straight lines detection. Vision parameters (gain, exposure time and aperture range), have been tested in this contribution in order to have a better visibility of the reference part. Tests were carried out by applying a rotation to the ceramic in five degree steps. The results show that with the *canny + hough lines* method, an accuracy of 99% is achieved. The proposed solution will be deployed in a Faurecia factory in order to validate the algorithm under real lighting conditions.
5. Having the plant autonomous is a key factor in the manufacturing industry. A solution has been developed by the Digital Expertise and Development (DE&D) service and aims at providing a Plug & Play system to the plants. This contribution will discuss the steps to be followed for deploying a digital solution in Faurecia's plants: integration of the solution in the plant's cycle time, architecture of the HMI, and implementation of the solution following the Innovation Program Management System (IPMS).

1.5/ DISSERTATION OUTLINE

The rest of this dissertation is organized as follows: chapter 2 discusses the product life-cycle in a Faurecia Clean Mobility plant and its quality control. Chapter 3 presents the state-of-the-art of neural network based computer vision and its applications in an industrial context. Chapter 4 presents the first contribution of this dissertation: the component presence control realized with ResNet50 deep learning model. Chapter 5 discusses the welding seam classification previously done manually by the operator, and integrates an automated solution with MobileNet architecture. Chapter 6 resolves the limitations

of the contribution presented in Chapter 5 by offering a hybrid deep learning approach. Chapter 7 applies image processing techniques to adjust brick orientation in the plants, avoiding by that potential defects and breakages. Chapter 8 presents the HMI used to integrate the computer vision contributions in Faurecia's plants. Chapter 9 concludes the work that has been done in this thesis.



INDUSTRIAL CONTEXT: QUALITY CONTROL IN
THE AUTOMOTIVE INDUSTRY

TYPES OF QUALITY CONTROL IN THE AUTOMOTIVE INDUSTRY

2.1/ INTRODUCTION

The goals of manufacturing activities include achieving product realization, establishing and maintaining a state of control and facilitating continual improvement. The quality system of manufacturing activities provides assurance that the desired product quality is routinely met, suitable process performance is achieved, and that the control sets are appropriate. One of the main responsibilities of manufacturing activities is to evaluate improvements of the production line. In this chapter, we will discuss the life cycle of a product in faurecia plants and the importance of automating factory procedures.

2.2/ PRODUCT LIFE CYCLE IN FAURECIA PLANTS

Confidential

2.3/ INDUSTRY AUTOMATION

The process of automated resources making actions at decision time without any human involvement is what we call automated decision-making. One of the crucial reasons for automating an industrial operation is worker safety. Heavy machinery, running at hot temperatures, and sharp objects increase the hazards of the factory environment. Another benefit of automation is freedom from fatigue. Machines can produce the same way the same part all day long without losing quality over time. Industrial automation does impact other parameters such as security, data integrity, interoperability, scalability, reliability, availability, and many others. Companies take a giant stride forward on financial

and technological aspects when they invest in manufacturing automation.

In agriculture [29], wood industry [40], robotic process [38], and many other fields, automation has proved its importance in accelerating decision-making. Automotive companies are also working on this automation and add a particular focus on quality automation to secure their processes. Instead of using the operator to control the quality of the reference part manually, an automated system needs to be deployed in order to verify the product's specifications.

2.4/ EXISTING SOLUTIONS IN THE MARKET

Following is the discussion the service Digital Expertise & Development (DE&D) had with an enterprise delivering quality control systems. Their quality control is focused on defects detection (dimensional control, aspect control and image classification), character reading (including distorted characters), and tracking with a robot (sending/receiving information from/to a personal computer).

The proposed system offers many advantages, such as providing deep learning model able to be trained with multi-classes. By that, multiple quality control applications can be gathered together in a single system. An other advantage is that this system has already been tested in a Faurecia plant and the network integration has been done in some plants. The information exchange between the provided system and Faurecia network is thus guaranteed.

Although the added value of this system is well identified, there are some disadvantages to take into account. Firstly, the price of the system bypasses the budget of the plants. Secondly, the system is fully delivered and treated as a package. It targets a quality control application and cannot be used for different types of quality control. Thirdly, the system does not cover remote access for maintenance. A physical move must be made in case of a breakdown of the system.

Due to the disadvantages presented above, Faurecia decided to develop its own automated system. The proposed system will guarantee the advantages of existing solutions in the market, and additionally it will provide the ability to cover different types of quality control in a single system.

2.4.1/ EXAMPLES OF QUALITY CONTROL

In this section, we will list some of the quality control types to be insured in the product's lifecycle. There are other types of quality control which we will discuss in more details in the next chapters.

GEOMETRY CONTROL

Confidential

SPATTERS CONTROL

Confidential

Confidential

Figure 2.1: OK sensor boss on the left, NOK sensor boss (spatters inside) on the right

CRACK CONTROL

Confidential

Confidential

Figure 2.2: Different types of end forming applied in the manufacturing industry

2.5/ CONCLUSION

We have presented, in this chapter, different phases of a manufacturing product starting with the truck reception area until the truck preparation area. Different types of quality control need to be applied throughout the product's lifecycle, and can be carried out manually or automatically.

A compromise should be defined between the speed of production and the various types of quality control. For that, manufacturing plants require automatized quality control in order to guarantee the quality of their products and maintain the same performance during different shifts. Automated solutions for quality control do exist in the market and able to provide high quality and sustainable performance. Given the inability to have a remotely accessible system, and a re-usable system to the different types of quality control, the DE&D service has developed a complete system. This system ranges from the computer vision (deployed algorithms) to the Human Machine Interface (HMI) to interact with the plant's operators.

In the next chapters we will be first presenting the state of the art of the neural network based computer vision. Then, we will continue listing the different types of quality control, in the contributions section, for which the DE&D service has adapted deep learning and image processing algorithms to automate them. And finally, we will present the HMI that has already been deployed in Faurecia plants, allowing the plants to be autonomous in terms of trace-ability and management of reference parts.

NEURAL NETWORK BASED COMPUTER VISION

3.1/ INTRODUCTION

Computer vision is an interdisciplinary field of artificial intelligence, evaluated and challenged by humans on a daily basis. It has proven its efficiency in problem solving in several areas: from automated farming to medical equipment, from global telecommunications to educational opportunities, from virtual reality to self-driving cars.

Among computer vision algorithms, many of them are based on neural networks. These algorithms have improved their performance compared to traditional image processing algorithms, especially in extracting useful information from images. In this chapter, we will go through the state of the art of computer vision based on neural networks. We will differentiate between artificial intelligence, machine learning and deep learning and we will discuss convolutional neural networks and some of their architectures. Lastly, we will present some of the image processing techniques used for analysing images.

3.2/ COMPUTER VISION DEFINITION

Computer science is the study of computers to solve problems. It employs theories on how computer work to design, test and analyze data. It includes hardware, human computer interaction, computational theory, vision and graphics, artificial intelligence, database systems, security and programming languages.

Computer vision is a field of computer science where computers can interpret and understand visual data: able to make decisions and take actions based on the data observed. Computer vision is applied for the benefit of different domains such as autonomous vehicles in the automotive industry, product assembly and defect detection in manufacturing, and many others.

3.3/ ARTIFICIAL INTELLIGENCE DEFINITION

Artificial Intelligence (AI) is a collection of theories and techniques implemented to make machines capable of simulating human intelligence, *i.e.* understand a text, compose music, move a player, One of the current applications of AI is machine learning, as represented in Figure 3.1.

Typical AI algorithms take actions to improve their performances, *ie.* during their learning phase, their parameters are progressively updated. The objective of an AI algorithm can be simple *ie.* predict housing price, and it can also be very complex, *ie.* learn to drive.

3.4/ MACHINE LEARNING

Machine learning is a discipline of artificial intelligence (as shown in Figure 3.1), that offers to computers the possibility to access to data and let them learn by themselves from a set of observations called a learning set. It is mostly applied for problems for which existing solutions require a lot of hand-tuning and for getting insights about complex problems and large amount of data. A machine learning system can adapt to new data and is able to be deployed in a fluctuating environment.

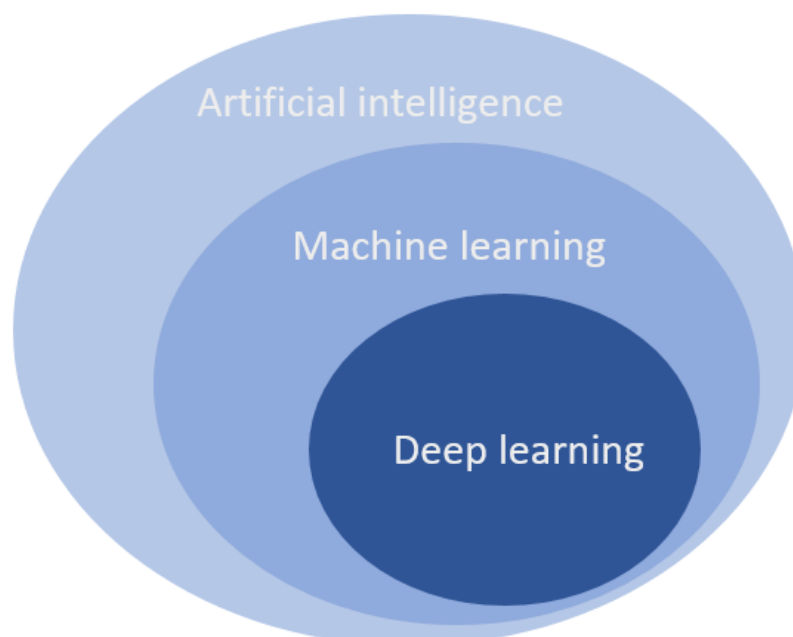


Figure 3.1: Artificial intelligence vs. Machine learning vs. Deep learning

3.4.1/ MACHINE LEARNING SYSTEMS

Three categories of machine learning systems are identified and can be listed as follows:

1. **Unsupervised learning:** this type of learning is most commonly used for analysing and classifying images in an unlabeled test dataset. It looks for instances, called outliers, that seem to fit least to the remainder of the dataset. Anomaly detection is an example of unsupervised learning.
2. **Supervised learning:** in this type of learning, data is fed to the algorithm and includes the desired solution. Labels are assigned to each input and distributed between classes.
The classification algorithm is an example of a supervised learning. It is used to predict discrete values for binary classification (*true or false, spam or not spam*), as well as for multi-classification (handwritten numbers: *one or two or three...*).
Another example of a supervised learning is the regression algorithm. It is used to predict continuous values. A very common type of regression is linear regression. It is used in statistics to quantify the relationship between a predictor and a response variable (*i.e. finding a relationship between business advertising spending and revenue*).
3. **Reinforcement learning:** the learning system (an agent) can observe the environment, selects and performs actions and gets returns: a reward is assigned to the agent if the action is relevant, whereas penalties can be allocated for irrelevant actions. It learns by itself what is the best strategy. DeepMind's AlphaGo program is an example of reinforcement learning [11].

3.4.2/ TYPES OF LEARNING

Two types of learning can be considered: batch and online. Batch learning systems, also called offline learning systems, are incapable of learning incrementally and thus require a lot of computing resources. As for online learning systems, their training phases are performed in an incremental way by providing input data sequentially, either individually or by small groups called mini-batches. Online learning systems are mostly used when computing resources are limited.

3.4.3/ CHALLENGES OF MACHINE LEARNING

Main challenges of machine learning are listed as follows:

1. **Bad data:** this means that the data used to train the model are either too few, non-representative, of poor quality or are displaying irrelevant features. The industrial context does not always allow a controlled environment: the defects vary and the data with defaults may not be always easy to collect. Thereby, dataset collection has to cover this diversity.
2. **Bad algorithm:** this results in overfitting or underfitting the training data. Overfitting is when the trained model is not able to perform well on new presented data. Underfitting the data is when the trained model is unable to capture the relationship between input data and output data. Thereby, the choice of the algorithm architecture and its parameters have to be adapted to each use case in order to prevent overfitting or underfitting.
3. **Imbalanced dataset:** it means that the input data classes are not evenly distributed: some classes are more represented than others. This problem is faced in binary class as well as in multi-class datasets.
4. **Noisy labels:** it corresponds to inaccurate or incorrect labels in the training datasets. The percentage of examples with incorrect labels in the dataset has a crucial impact on model performance.

In order to get a clear idea of the accuracy of an AI model, many methods can be tested. One of these methods is the *Confusion matrix*.

3.4.4/ CONFUSION MATRIX

Confusion matrix is a method that allows to measure the performance of an AI model. It displays how many categories or classes were correctly predicted and how many were not.

An example of a confusion matrix is shown in Figure 3.2. The rows in the confusion matrix correspond to what the machine learning algorithm learned, while the columns correspond to the known truth.

Parameters of a confusion matrix are usually expressed in percentage or in numbers. Following are the four identified parameters and an example of each parameter in a self driven car scenario:

1. **True positive:** is an outcome where the model correctly predicts the positive class (*ie.* there is a pedestrian and the model says that there is a pedestrian).
2. **True negative:** is an outcome where the model correctly predicts the negative class (*ie.* there is no pedestrian and the model says that there is no pedestrian).

3. False positive: is an outcome where the model incorrectly predicts the positive class (*ie.* there is no pedestrian but the model says that there is a pedestrian).
4. False negative: is an outcome where the model incorrectly predicts the negative class (*ie.* there is a pedestrian but the model says that there is no pedestrian).

In Figure 3.2, the top left corner, contains the true positives. The true negatives are in the bottom right-hand corner. The bottom left-hand corner contains the false negatives. Lastly the top right-hand corner contains the false positives.

The numbers along the diagonal tell how many times the samples were correctly classified. The numbers not on the diagonal are samples the algorithm messed up.

When comparing two confusion matrix of two different AI models trained on the same dataset, the best model is the model having the highest percentage of true positive and true negative.

		True class	
		Positive	Negative
Predicted class	Positive	True positive	False positive
	Negative	False negative	True Negative

Figure 3.2: Confusion matrix of an AI model

3.5/ DEEP LEARNING

Deep learning (DL) is a subcategory of machine learning (as shown in Figure 3.1). These algorithms are particularly effective when the human brain is efficient too, for example object recognition using a picture, or in transcribing a discussion into text. These algorithms work by simulating neural networks, thus mimicking the functioning of the brain (a network of neurons).

There are many types of DL models, and each is suitable for different contexts. For example, Convolutional Neural Networks (CNN) are very effective in topics related to vision, Recurrent Networks (RN) are more effective at transcribing speech to text [70], and

Generative Adversarial Networks (GAN) are able to create new images [64].

3.5.1/ CONVOLUTIONAL NEURAL NETWORK

DL models have achieved promising results in detecting the difference between two images. These algorithms are used in the classification of images to prevent any bad decision making. One of the most popular DL architectures is the CNN.

The output signal strength of a CNN is independent of where the features are located, but simply whether the features are present or not. For example, in an alphabet classification, the character could be sitting in different position and the CNN would still be able to recognize it.

3.5.2/ CONVOLUTIONAL NEURAL NETWORK APPLICATIONS

CNN has proved to be very efficient in extracting deep features [26, 17, 16]. The architecture of a CNN, based on a succession of layers, reduces images without losing the important features, which leads to getting good prediction. Each layer transforms the input volume to an output volume. CNN performs well on a series of visual applications and tasks, such as image classification [49, 28, 30], image detection [35, 42, 22] and image denoising [45, 46, 27].

CNNs have been applied on manufacturing use case and proved their adaptability to the environment's conditions [62, 63, 77]. In a binary classification, where the dataset is composed of two classes, a CNN will learn the specific features of a class. Once the learning phase is done, the output model will be able to predict if the given image belongs to the first or the second class.

3.5.3/ HOW CONVOLUTIONAL NEURAL NETWORKS WORK

Each image is divided in three channels: red, green and blue. For each pixel, a value is assigned to each of these channels. The computer is able to recognize them and identifies the image size. Four steps can be identified in a convolutional neural network architecture:

1. Convolution: this step consists on browsing the image with a filter. Each pixel is multiplied by its corresponding value in the filter. The result is a buffer with a size equal to the filter's size. The filter is then moved around and the same procedure is done at any pixel in the image.

Figure 3.3 shows the parameters of the convolution phase, from left to right: *Image*, *Kernel*, and *Convolved feature*.

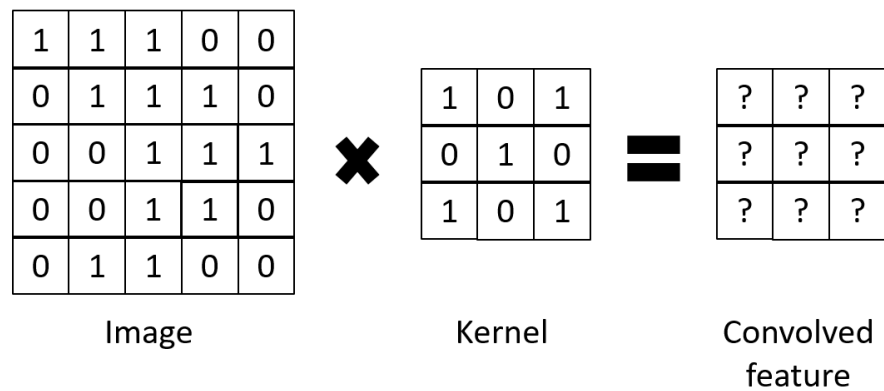


Figure 3.3: Convolution phase: parameters

An example of the first convolution step is represented in Figure 3.4. The kernel is placed on the top left of the image. Each pixel is multiplied by its corresponding value in the kernel. The sum of all of these coefficients is then added in the convolved feature.

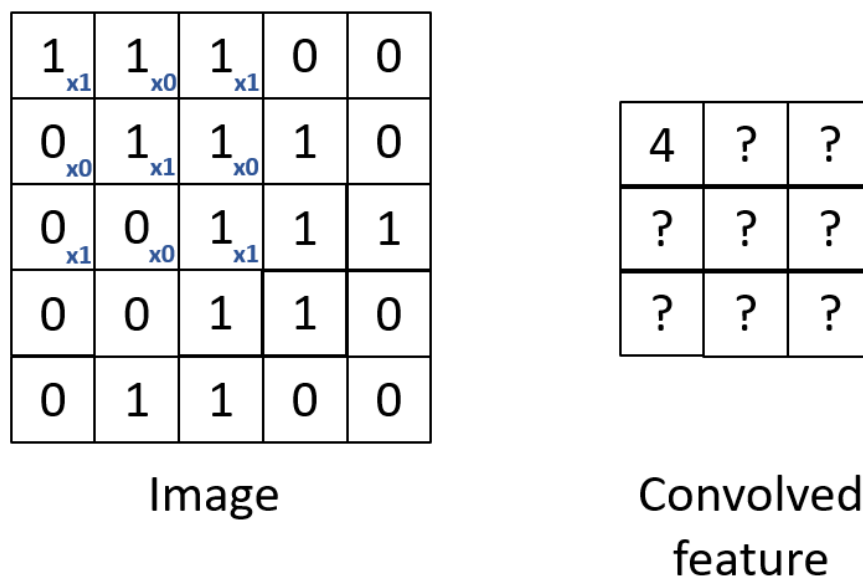


Figure 3.4: Convolution phase: Step 1

The second step of the convolution is represented in Figure 3.5, on the left. In this step, the kernel has been moved one pixel to the right. As in the first step, each pixel is multiplied by its corresponding value in the kernel and the sum of all of these coefficients is then added in the convolved feature.

The third step is when the kernel is moved again to the right and same calculations of the previous steps are applied. In the fourth step, according to Figure 3.5 on the right, the kernel has been moved to the second line and so on.

An example of the final step obtained at the end of the convolution phase is repre-

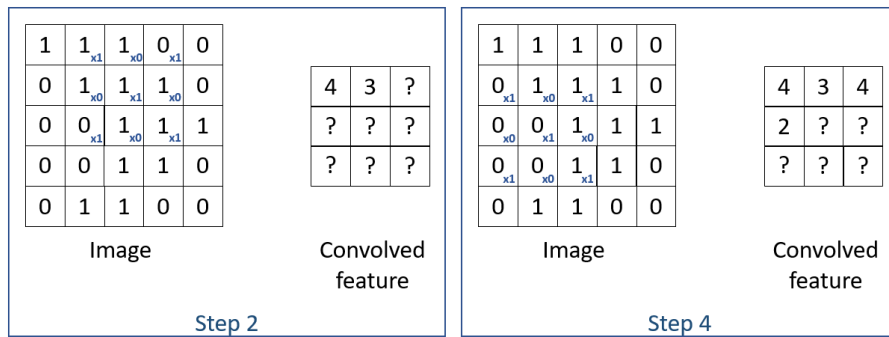


Figure 3.5: Convolution phase: intermediate steps

sented in Figure 3.6. Each element of the convolved feature has been assigned a value.

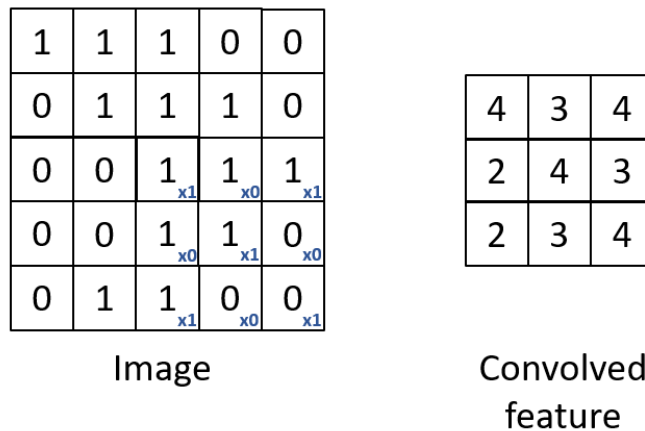


Figure 3.6: Convolution phase: step 9 (last step)

2. **Activation function:** it is applied on a node and determines its output given an input or set of inputs.
 ReLU: Rectified Linear Unit is an example of an activation function. It only activates a node if the input is above a certain quantity: while the input is below zero, the output is zero, but when the input rises above a certain threshold, it has a linear relationship with the dependant variable.
 In Figure 3.7, different types of activation functions are represented, such as: *Tanh*, *ReLU*, *Sigmoid*, and *Linear*.
3. **Pooling layer:** pooling layers are used after the convolutional layers to order layers that may be repeated several times in a single model. By that, the number of parameters to learn from and the computation complexity are reduced. This reduction makes the model more robust to variations of the features' positions. An example of a max pooling phase and an average pooling phase are shown in Figure 3.8. The stride is equal to 2 and a result of 2x2 pooling is obtained.

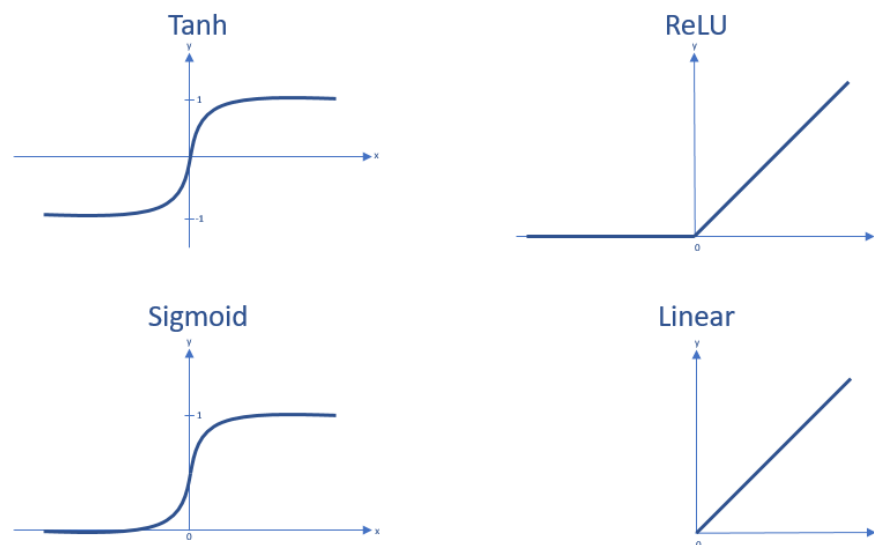


Figure 3.7: Activation functions applied in deep learning

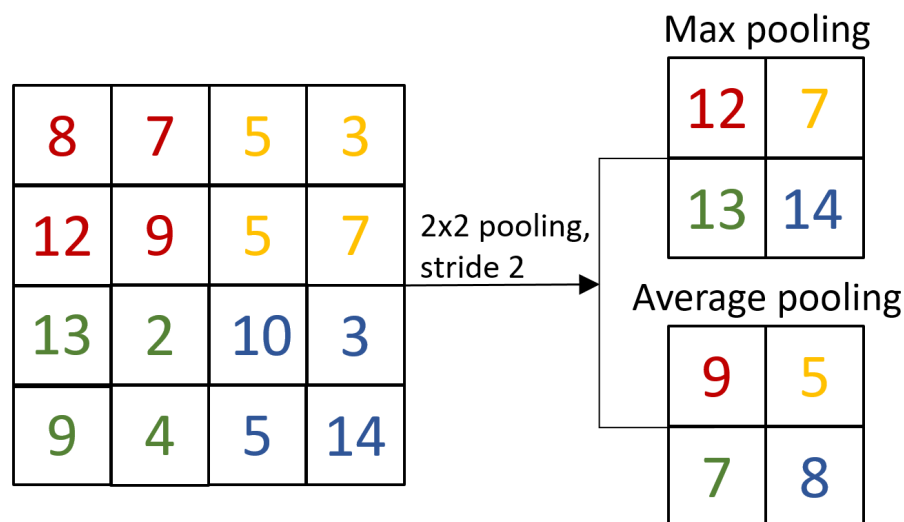


Figure 3.8: Pooling phase

4. Fully connected layer: in this step, the last layers in the network are fully connected, meaning that neurons of preceding layers are connected to every neuron in subsequent layers. The classification happens in this step.
5. Retro-propagation: characteristics and weights are adjusted to reduce the error when repeating the cycle of the four steps presented above (convolution, activation function, pooling, and fully connected layers). Each value is increased or decreased, and the new network error value is recalculated, with each iteration. Regardless of the adjustment made, if the error decreases, the adjustment is retained.

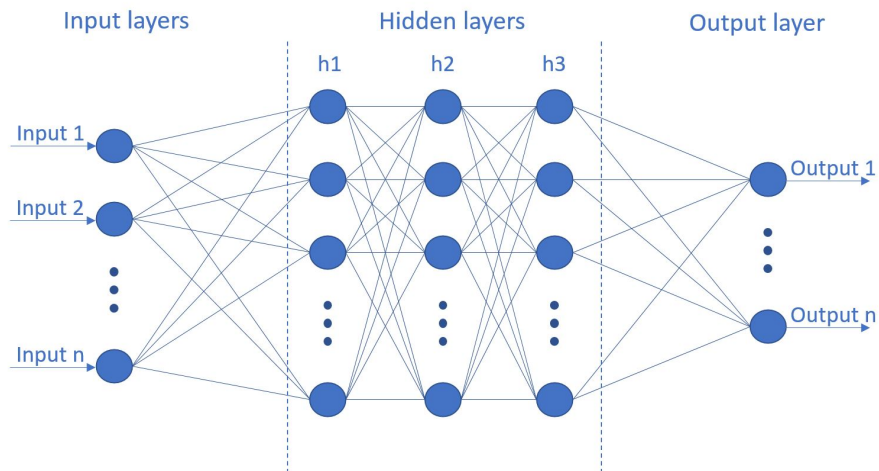


Figure 3.9: Neural network architecture

3.5.4/ STEPS TO DESIGN A NEURAL NETWORK

The global steps to train a neural network are identified as follows:

1. **Data collection:** images for both classes are collected; whether collected from an online dataset or live images collected from a specific use case.
2. **Data cleaning:** data's verification is done in this phase. Biased images should be removed. If there is any need to apply specific filters or crop before training the model, these steps should be applied in this phase.
3. **Training phase:** extract features from images while training the model. As shown in Figure 3.9, the neural network receives an input and assigns a weight to it. Then, transmits it to hidden layers until reaching the output layer. The existing layers are interconnected between each others in order to extract features. These features are then distributed between different classes, each class representing an output.
4. **Validation phase:** To deliver an output, the model is tested on input that have not been trained. At the end of each iteration, the model adjusts its weights based on the data used for validation. It allows to evaluate the current state of the learning phase in terms of accuracy and loss.

3.6/ CNN ARCHITECTURES

Some CNN architectures have proven their efficiency when applied in an industrial context. In this section, we will be discussing two of these applications and their architectures: *ResNet50* and *MobileNet*.

3.6.1/ RESNET50 APPLICATIONS

Mangalam *et al.* [15] have invested in ResNet50 for bird call recognition. Spectrograms (visual features) extracted from the bird calls were used as input and were able to achieve 60 to 72% of birds call recognition.

Jiang *et al.*[31] have worked on detecting and classifying Floral disease. The database includes images of the leaves of the affected plants. This classification is done using a neural network that requires 900 images per class and uses the Resnet50 architecture. The results obtained reach a disease detection percentage equal to 98%.

Rezende *et al.* [8] applied ResNet50 to classify malicious software. Malware samples were represented as byteplot grayscale images and were provided to the input layer. The experimental results reached an accuracy of 98.62% for classifying malware families.

Theckedath *et al.* [44] investigated in 3 architectures: VGG16, ResNet50 and SE-ResNet50. This method reuses weights of already developed models to train a CNN and detects 7 basic affect states. The evaluation shows that ResNet50 outperforms other networks reaching a validation accuracy of 99.47%.

Wen *et al.* [19] is an example where ResNet50 is applied in the manufacturing domain. The dataset includes bearing damage, motor bearing, and self-priming centrifugal pump dataset. By adding one layer in order to transfer time-domain fault signals to RGB images format as input for ResNet50, the prediction accuracies reach around 99%.

3.6.2/ RESNET50 ARCHITECTURE

ResNet50 has 48 convolution layers along with one average pool layer and one fully connected layer. ResNet50 uses shortcut connections which ensures that the higher layer will perform at least as good as the lower layer, and not worse. The input is an image tensor. Each three convolution layers forms a block called bottleneck block. The input of each block is added to the next block, thereby a shortcut connection (or skip connection) is created. Figure 3.10 illustrates how layers communicate with each other.

The dotted lines refer to a change in the dimension of the input that is needed. For example, if the number of channels of the previous layer is equal to 256 and the next one is equal to 512, a change of the number of channels of the previous basic block should be applied in order to be equal to the next block. In this case, it should be multiplied by 2. Finally, the average pooling and fully connected layers are added. Average pooling means downsampling the feature map (output of one filter applied to the previous layer) by calculating the average of each patch of the feature map (2x2 square). Then, the fully connected layer flattens the output of the average pooling, going through its backpropagation process in order to define the most accurate weights.

Following are the details of each and every block: a block takes an input to perform

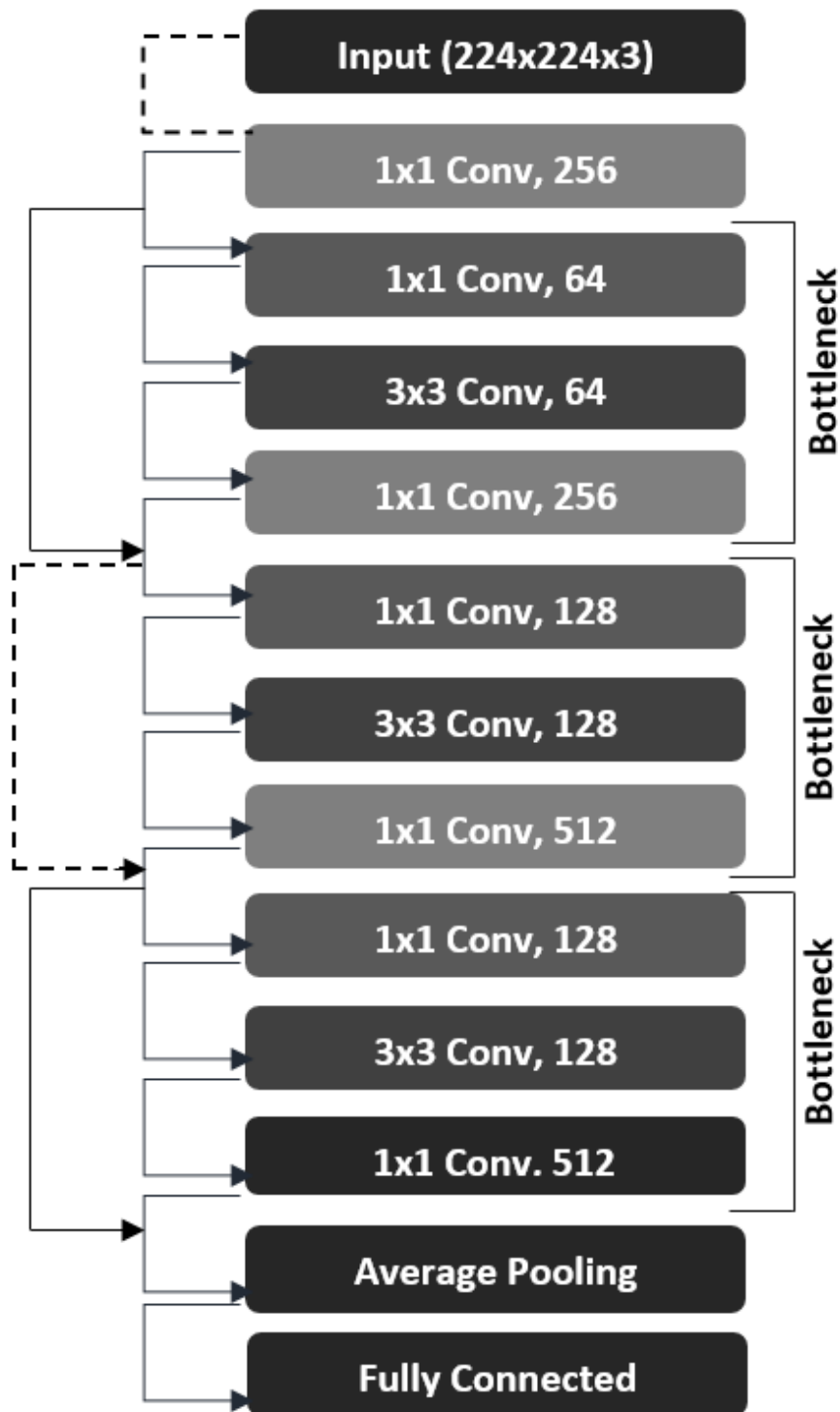


Figure 3.10: Skip connection and bottleneck in ResNet50 Architecture

convolution, produces an output, and then activates the output. It will repeat this same procedure for the second and the third block. On the other hand, for the second and third block, to activate the output, the same input is added, and then the output is activated. So, instead of adding convolution layers to improve accuracy, ResNet adds, skip connec-

tions.

In the following sections, we will be talking about the MobileNet CNN, its applications and architecture.

3.6.3/ MOBILENET APPLICATIONS

MobileNet architecture proved its efficiency when applied on different domains [61, 72, 53], by constructing lightweight deep convolutional neural networks.

Pan *et al.* [37] proposed an example where MobileNet is applied to ensure the quality of the weld structure. They proposed a new transfer learning model based on the MobileNet architecture by adding a new Full Connection layer and a Softmax classifier. This method has been tested on the welding defects dataset and the model is able to reach an accuracy of 97.69%.

3.6.4/ MOBILENET ARCHITECTURE

In a traditional CNN, the input is an image following this format: $S = s \times s \times c$, where S is the size of the image in bytes, s is the width and height of the image, and c its number of channels (equal to 3 for an RGB image).

MobileNet separates the convolution phase in two smaller parts:

1. Depthwise convolution : having the same image as input with size $S = s \times s \times c$, the kernel size remains the same ($n \times n$) but this time, the kernel iterates only one channel of the image. The output is an image with size s_1 where $s_1 = s - n + 1$ with $depth = 1$.
2. Pointwise convolution: this convolution takes place after the depthwise convolution. In this case, the kernel has a size s_k , where $s_k = 1 \times 1 \times c$. The output of this convolution is an image with a size s_1 where $s_1 = s - n + 1$ with $depth = 1$. Then, this kernel is applied f times in order to obtain f number of feature maps.

Image processing techniques remain robust techniques for analysing images. In the next section, we will present some applications where image processing were applied for highlighting edges either with the canny filter or the laplacian edge detector.

3.7/ IMAGE PROCESSING

Some of the applications for detecting edges with image processing can be listed as follows:

1. Detection of retinal disease: diabetic retinopathy is highlighted by detecting the contour of the fundus[54]. This method transforms RGB images into grayscale images. The canny edges approach will be applied to the latter in order to highlight the contours of the eyes and to detect the disease.
2. The detection of traffic lanes by means of a camera installed inside the vehicle was carried out by Rossi et al. [39]: canny edges and Hough lines algorithms are applied to detect traffic lanes.
3. The detection of bladder cancer by image processing using the Laplacian edges detector algorithm was carried out by Lorencin et al. [33]. This method allows areas of interest to be highlighted and achieves an accuracy of 99% on nearly 3000 images.

3.8/ CONCLUSION

In today's manufacturing industry, AI is being applied in many applications to automate systems and processes. In this chapter, we have covered the state of the art of CNN-based computer vision and have seen its efficiency when applied in industrial applications. In the next chapters, we will put these advancements in an automotive context. For quality control to be automated, it is not only necessary to achieve the precision required by the customer, but it is also necessary that this response be provided within a time frame suitable for the cycle time of the production lines. Types of quality control studied in this thesis are component presence control, welding seam classification and brick orientation adjustment. The quality control to be automated will be based on the state of the art drawn up above.



CONTRIBUTIONS

COMPONENT PRESENCE CONTROL IN THE AUTOMOTIVE INDUSTRY USING DEEP LEARNING

4.1/ INTRODUCTION

This part examines the main contributions in this thesis. As discussed in the previous chapters, the proposed approaches and methods are designed to solve different challenges in the data collection and data processing phases of an artificial intelligence application deployed in industry.

In modern factories, especially in the transportation industry, factories often have to produce a vast number of different references. Within each reference, some functional part dimensions may show dissimilarities. For that, quality control is necessary and should be applied to every reference part. Several technologies are used such as visual & geometric control, leak test, and many other functional tests. Today, the implementation of these tests is expensive, whether because of the necessary tools or the manpower. Visual control is done by the operator who checks each part manually, making the reliability highly improvable. At first, the automation of the inspection can be carried out by different methods: camera, thermography, laser scanning, and in conjunction with artificial intelligence techniques [26, 19]. Then, it will be necessary to correlate these quality results with different parameters (processing and environmental) to reduce non-conformities.

The main goal of this contribution is to provide automatic control of the manufactured products in the automotive industry by detecting the presence or absence of a component and to overcome the need for human intervention. This quality control needs to be done primarily to assembling the exterior part of the car because once these two parts are joined, the component may not be accessible anymore.

Our contribution will help the current state of manufacturing by offering an automatic visual inspection, which will lead to other innovative projects in the automotive industry.

4.2/ PROBLEM STATEMENT

Figure 4.1 is an example of a sub-assembly that takes place in the vehicle. The presence or absence of 10 screws of three different models, respectively called *Rivstud*, *Rivnut* and *Flexitol*, each in its own region of interest, should be checked. In the Figure, the regions of interest are presented with their right screws.

The component control should be done while taking into consideration the different lighting conditions of the plant.

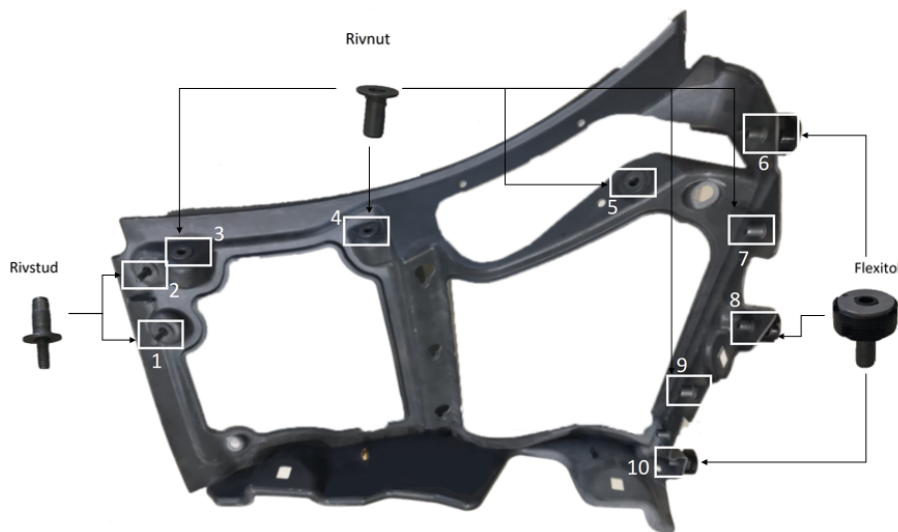


Figure 4.1: Sub-assembly part to be checked. The three types of screws and their expected locations are displayed by the means of the black arrows.

The same type of screw may be the right one for a specific region of interest and the wrong screw for another region. Three possibilities can show up:

1. The right screw is present in the right region of interest.
2. The screw is missing.
3. There is a screw, but not the one we expected. This case is considered as NOT OK (NOK).

The reference part is OK if the first possibility, defined above, has been identified on all of the ten regions of interest. The reference part is NOK if one of the ten regions of interest is assigned to the second or third possibility. In this case, the reference part should be sent to rework.

4.3/ AUTOMATIC CONTROL IMPLEMENTATION

4.3.1/ DATA COLLECTION

All images have been collected in the plant during multiple shifts to cover different lighting conditions. The camera used is an 18MP device, positioned above the part at a distance of 500mm. The image size has a length of 4912 pixels and a width of 3684 pixels. Each global image is split into ten small images, centered on the ten regions of interest (each cropped image has a length varying between 200 and 400 pixels and a width varying between 150 and 250 pixels). The coordinates of each region of interest were defined prior to cropping. With 1920 global images obtained from the plant, the data set contains a total count of 19200 cropped images. Among these 19200 images, we randomly selected 70% of them for the model training, 20% for the model validation and the remaining 10% for the testing phase.

4.3.2/ ANALYSIS OF THE COLLECTED DATA

Based on the collected data, some regions should have the same type of component and look the same for the camera. As shown in Figure 4.1, the *rivstud* model is expected in regions 1 and 2. These two regions look the same for the camera.

For some other regions, the same component is expected, but look totally different for the camera, according to Figure 4.1. These similarities help in grouping some regions and allow associating the most possible images to a specific class. These common areas are grouped in four categories:

1. **Category 1:** contains regions 1 and 2.
2. **Category 2:** contains regions 3, 4 and 5.
3. **Category 3:** contains regions 6, 8 and 10.
4. **Category 4:** contains regions 7 and 9.

As displayed in Figure 4.2, each line represents a category and each column represents a component model. Categories are divided into four different classes according to the different possible cases. For example, images from Category 1 are split as follow: *Category1-flexitol*, *Category1-rivstud*, *Category1-rivnut*, *Category1-missing*. The class *Category1-missing* represents the images where none of the components is present in Category 1.

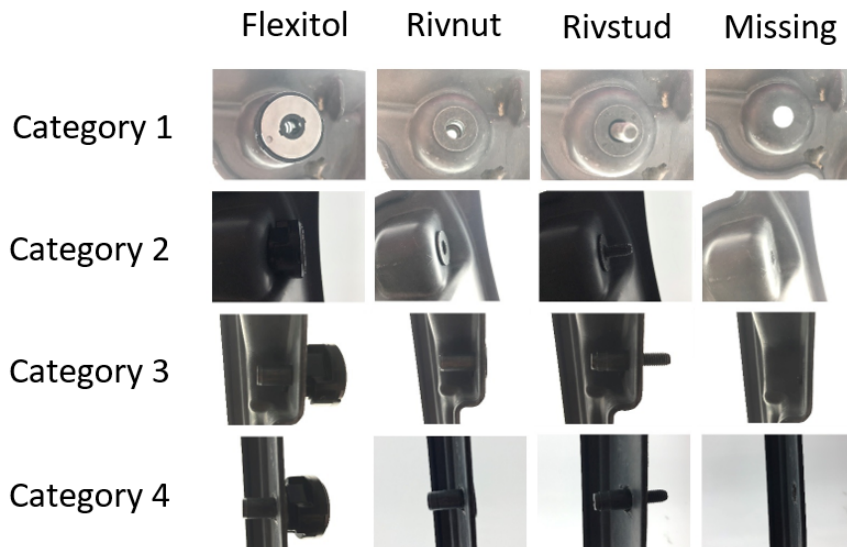


Figure 4.2: Sample of each class in the trained model

4.3.3/ EXPERIMENTAL ENVIRONMENT

The experimental environment is powered by Intel i5 CPU with 64-bit Windows 10 operating system, a memory of 8 GB, and 2.30 GHz basic frequency. The software programming environment is python. It is based on Keras framework, having Tensorflow and Theano as backend.

In the image classification model, Adam is selected as an optimizer of the CNN. The learning rate is set to 10^{-5} . Concerning the ResNet50 weights, a pre-trained version of the network, trained with the ImageNet database has been loaded.

The input of the CNN is a 4D array. It has a shape of (batch size, height, width, depth). The batch size (equal to 32 in our case) defines the number of samples that will be propagated through the network. The other parameters represent the height, width, and depth of the image. In our case, the input has the following values (32, 224, 224, 3). The model has been trained with 100 epochs. Each epoch passes the entire data set through the neural network, only once.

4.4/ EXPERIMENTAL RESULTS

4.4.1/ ACCURACY IMPROVEMENTS

Our approach for sub-assembling family classification is assumed from a CNN model based on the Residual Network architecture with 50 layers (ResNet50), presented in chapter 3.

Table 4.1 shows that the accuracy reaches 100% with our deep learning model. The

software is able to detect not only the presence or absence of the component but also the presence of a screw of the wrong type.

Table 4.1: Accuracy comparison between human-being check and ResNet50

Component type	Human-being check(%)	ResNet50-offline(%)
flexitol	98	100
rivstud	97	100
rivnut	98	100
missing	93	100

Comparing the results between the human-being check and the autonomous control of ResNet, an upgrade of the average precision is noticed from 96.5% to 100.0% respectively (as presented in Table 4.1). These results show that replacing the human-being check by an automatic visual inspection system provide better accuracy.

4.4.2/ CYCLE TIME AND RELIABILITY IMPROVEMENTS

Ten operators have been chosen randomly (having five to twenty five years of experience) and have been given an OK part (containing all 10 regions with their right screws). It is easier for an operator to make the visual inspection of an OK part than inspecting a NOK part. Moreover, this same part has been processed with the ResNet50 neural network architecture. The test was repeated ten times.

As in Table 4.2, the average time spent by operators to check this part ranges from 6 to 8 seconds depending on the operator, while the average execution time of the neural network with this same part is around 5 seconds. The neural network provides a stable performance, it will not be affected during the day. The total execution time decomposes as follow: ResNet50 needs 0.4 seconds per region and the cropping of all 10 regions needs 1 second.

When evaluating a NOK part, an operator has to consider four different possible situations for each region of interest. That leads to increase the average human inspection time for NOK parts. At the opposite, we are sure that the ResNet50 will run in 5 seconds. Cycle time is then improved with the automated visual inspection.

In addition to these two parameters, we must take into account the overall equipment effectiveness (OEE). Its calculation is based on three factors:

- 1. Availability:** it concerns the events that stopped planned production long enough, and need to track a reason for being down.
- 2. Performance:** it concerns anything that causes the industrial process to run at less than the maximum possible speed when it is launched.

Table 4.2: Cycle time's comparison between human-being check and ResNet50

Operator \ Test	time (in seconds)					Average
	Test 1	Test 2	Test 3	Test 4	Test 5	
Operator 1	9.24	8.40	8.67	9.45	8.22	8.796
Operator 2	9.85	8.63	8.19	9.03	8.15	8.770
Operator 3	8.40	7.29	7.01	7.46	7.58	7.548
Operator 4	7.56	7.77	7.65	6.54	7.18	7.340
Operator 5	8.74	9.52	7.20	7.33	8.42	8.242
Operator 6	6.48	5.88	6.39	5.91	6.02	6.136
Operator 7	8.85	9.32	8.66	9.27	8.33	8.886
Operator 8	8.58	9.08	9.25	8.85	8.19	8.790
Operator 9	8.72	7.48	7.56	7.37	8.11	7.848
Operator 10	7.36	7.82	8.66	7.44	8.23	7.902
ResNet50	5.21	5.42	5.08	5.28	5.39	5.276

3. **Quality:** it considers *good parts* as parts that successfully pass through the manufacturing process the first time without needing any rework. By that, it takes into account all manufactured parts that need rework. It is calculated as the ratio of *Good Part Count* to *Total Part Count*.

With our proposed model, OEE is clearly enhanced. Firstly in terms of performance: reducing the number of operators for the visual inspection increases the reliability. This is due to the fact that the algorithm will avoid performance degradation over the operator's shift.

On the other hand, better quality is reached: by detecting defective parts at an early stage before being assembled with others. This increases the percentage of good parts passing through the manufacturing process for the first time without needing any rework. Controlling presence or absence in automotive industry is not needed for screws only. Many topics need quality control such as welding, spatters, holes, and many others. The proposed solution can be tested on these different topics and may be applied safely in plants.

4.5/ CONCLUSION

We proposed a method based on deep learning to control component presence. The features of the dataset are extracted by ResNet50, which fully achieves the ability to extract images' features. The results show that the maximum accuracy of the proposed method is 100%, which can meet the requirements for visual inspection in the production line. The images collected as data set for classification have been all carried out offline. After the required accuracy is reached, new images were taken in the actual industrial production.

The model tested on these images reached 100% accuracy. Thereby, the effectiveness and practicability of the proposed model are verified by the plant. Results show that the automation of quality control in the automotive industry does improve reliability, accuracy, and cycle time.

In our future work, we plan to detect object movement and being able to readjust the camera's angle in order to increase the flexibility and the robustness of this system. In other words, a self-adjusting system regardless of environmental disturbances.

WELDING SEAM CLASSIFICATION IN THE AUTOMOTIVE INDUSTRY USING DEEP LEARNING ALGORITHMS

5.1/ INTRODUCTION

Welding is one of the processes that allow to connect two pieces of metal together. Many industries use welding to connect parts of their products. For example, in the aviation industry [76], welding is used in the manufacturing and maintenance processes of aircrafts. It requires lightweight components and flawless welds to comply with safety standards before taking off to the skies.

Welding is also employed in the construction of buildings, where the creation of the structural frameworks is based on metal components. Thereby, it is used to support walls, roof and floors of many buildings.

In the automotive industry, robustness of the welds and leakage absence are highly required. A discontinuity in a welding seam may have a huge impact on the quality of the product, thereby on client's satisfaction. That is why welding seam inspection is done at each step of the assembly process.

The most fundamental reason for inspecting a weld is to determine whether its quality reaches the requirements for its intended application. If the weld is identified as deficient (NOK), rework should be applied on this weld.

Acceptance criteria should be defined when measuring the two main characteristics of a specific weld: its size and the presence of discontinuities. In order to prevent weld failure due to these defects, a welding inspection is necessary and should be done right after the welding phase.

In order to validate the automatic welding seam inspection, it should be able to reach high precision in detecting defective parts: reaching 97% of accuracy when applied on NOK

parts, as requested by the client.

5.2/ WELDING SEAMS IN THE AUTOMOTIVE INDUSTRY

5.2.1/ TYPES OF WELD JOINTS

According to [82], weld joints can be classified as follows:

1. **Butt joint:** a joint where two pieces of metal are placed together in the same plane and the side of each metal is joined by welding. This is the most common type of joints used in the fabrication of structures and piping system. Many different variations can be applied to achieve the desired result. They are made in a variety of ways and each one serves a different purpose. Varying factors include the shape of the groove, the layering and the width of the gap. As shown in Figure 5.1, there are different types of butt joints, such as: *Square*, *Single bevel*, *Single V*, *Double bevel*, *Single U* and *Single J*.

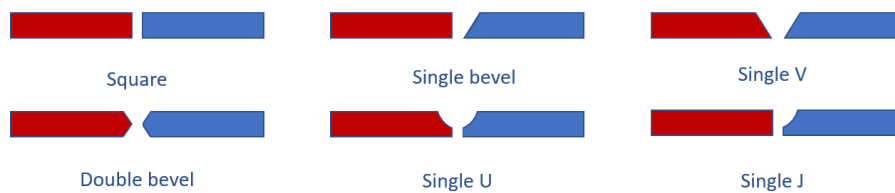


Figure 5.1: Butt joint types

The area of the metal surface that is melted during the welding process is called the faying surface. It can be shaped before welding to increase the weld strength which is called the edge preparation. The edge preparation may be the same on both members of the butt joint or each side can be shaped differently.

2. **Tee joint:** it is formed when two pieces intercept in a ninety degrees angle. This results when the edges are coming together in the center of a plate or a component of a T-shape. Tee joints are considered as a type of a filled weld and they can also be formed when a tube or a pipe is welded on a base plate. There are different types of tee joints, as shown in Figure 5.2 from left to right: *Plug*, *Bevel groove*, *Fillet*, and *Flare-bevel*. The most used tee joints at Faurecia are *Fillet*, and *Flare-bevel*.
3. **Corner joints:** they have similarities with Tee welding joints. However, the difference is the location of where the metal is positioned. In Tee joints, it is placed in the middle, whereas in corner joints it meets in the corner in either an open or closed manner forming an L shape. Figure 5.3 represents two types of corner joints, from left to right: *Spot* and *Fillet*. These types of joints are among of the most common

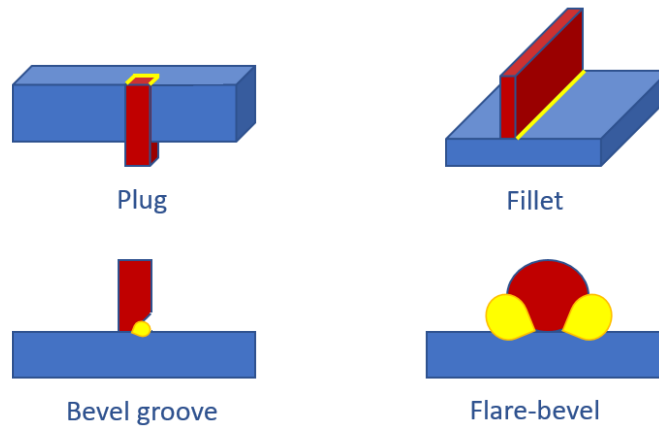


Figure 5.2: Tee joint types

in the sheet metal industry such as in the construction of frames, boxes and other applications.

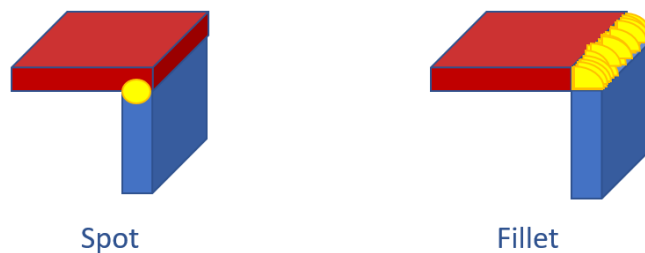


Figure 5.3: Corner joint types

4. Lap joint: they essentially are a modified version of butt joints. They are formed when two pieces of metal are placed in an overlapping pattern on top of each other, as shown in Figure 5.4. They are most commonly used to join two pieces with different thickness together. Welds can be made on one, or both sides. Lap joints are rarely used on thicker materials and are commonly used for sheet metal.

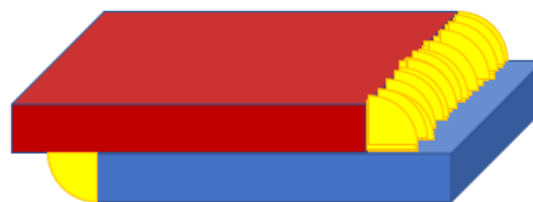


Figure 5.4: Lap joint example

5. Edge joint: the metal surfaces are placed together so that the edges are even. One of both plates may be formed by bending it at an angle, as represented in Figure 5.5.

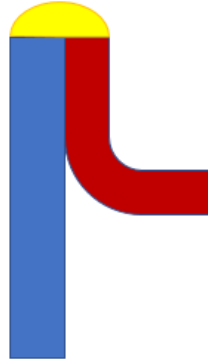


Figure 5.5: Edge joint example

5.2.2/ TYPES OF WELDING TECHNOLOGIES

As represented in Figure 5.6, and according to [83, 84], welding seams can be classified as follows:

1. Metal Active Gas (MAG) welding: fusion welding process uses an electrical arc between a continuous filler metal electrode and the weld pool. The process incorporates the automatic feeding of a continuous, consumable electrode that is shielded by an externally supplied gas.
2. Tungsten Inert Gas (TIG) welding: fusion welding process, that uses an electrical arc between a non-consumable tungsten electrode and the work piece to create the weld pool. The process may incorporate filler wire and is shielded by an externally supplied gas.
3. Plasma Arc Welding (PAW): fusion welding process, that uses an electrical arc between a non-consumable tungsten electrode and the work piece to create the weld pool. The tungsten is recessed into the torch and a constricting nozzle is used to restrict the arc into a narrow column. The process may incorporate filler wire and is shielded by an externally supplied gas.

In this contribution, we will focus on MAG welding. The target is to alert if the welding is NOK or not at the end of each operation. The size of the inspected welding seams ranges between 50 and 60 mm.

5.2.3/ TYPES OF WELDING SEAMS QUALITY CONTROL

In this thesis context, the quality control of welding seams is applied on exhaust systems. Welding joints are thus evaluated as follows:



Figure 5.6: Types of welding technologies

1. Visual control of the external appearance (non-destructive): in this type of quality control, the weld must be completed according to drawing specifications, no missing sections or interruptions are allowed. A circular weld may not have a constriction at the overlap.

Other welding defects to be inspected such as burn through or holes, visual fusion defects (*ie.* weld misses one or more of the components locally and completely, cold weld) are not allowed. Examples of a welding seam considered as OK, as well as welding seams considered as NOK, are shown in Figure 5.7.

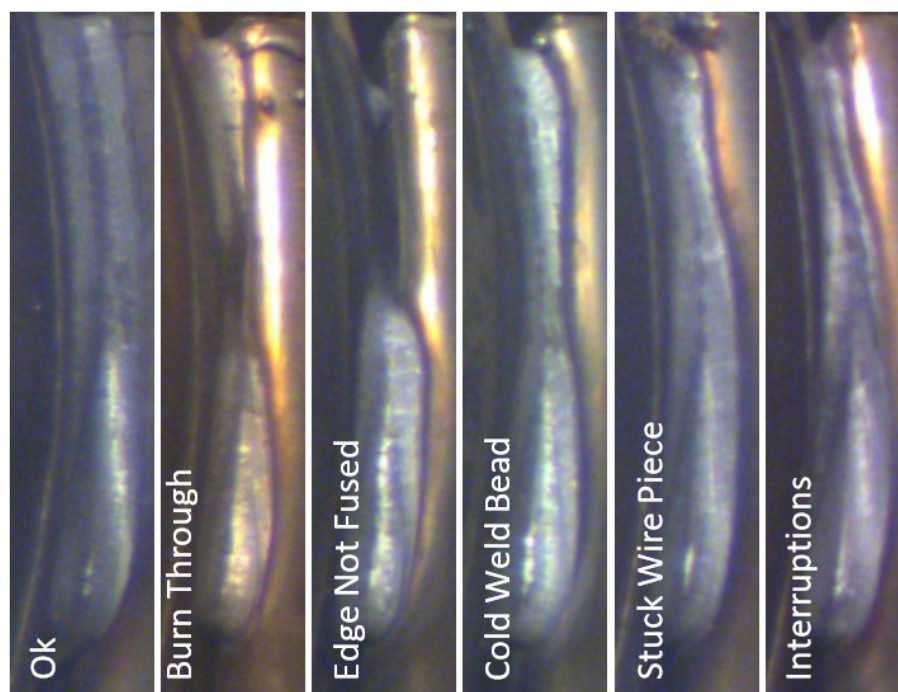


Figure 5.7: Reference weld (OK) and five possible defects (NOK) for MIG/MAG welding

2. Evaluation via cut & etch samples (destructive): a weld sample is cut out perpendicularly to the weld with a smooth or polished plane, as in Figure 5.8. The smooth plane is etched to show the fusion boundaries. Cut & etch samples are evaluated

with an optical magnification of at least 8-fold. These samples are cut out at a position of minimum 10 mm measured from the weld start and end point on welds longer than 20 mm. On welds shorter than 20 mm, the section is taken on the half of the weld length.

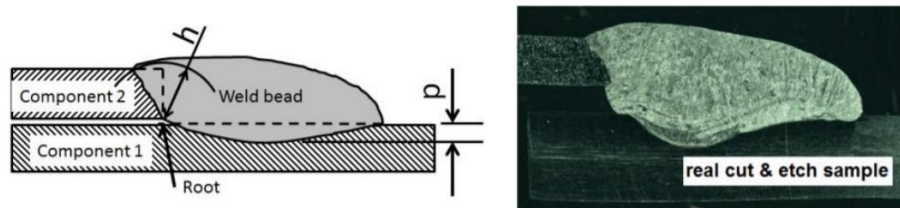


Figure 5.8: Effect of MIG wire feed speed on the welding tested by cutting and etching

3. Measurement of weld lengths (non-destructive): when measuring the weld length, one must consider two types of weld beads: a so-called linear weld (where both ends are not on the same position) and an all-around weld, where there is an overlap at start and end. The length of an all-around weld does not have to be measured. As represented in Figure 5.9, the weld length is to be measured as the distance between the visible weld bead's start and end along the virtual weld bead center line while compared to the length specified on the drawing. If the measured length is equal to or greater than the length specified on the drawing, then the weld bead length is in conformance. In this contribution, we are working with welding seam size ranging between 50 and 60mm.

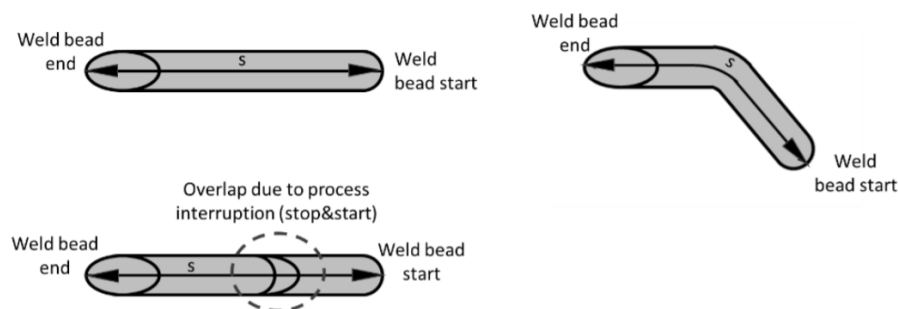


Figure 5.9: Measurement of the weld length

The focus of the proposed quality control is on automating the visual control of the external appearance.

5.2.4/ WELDING SEAMS INSPECTION

Visual inspection is a necessary operation for manufacturing industries [48, 41, 25]. As displayed in Figure 5.10, its main function (MF1) is to visually check a product during its production process. Many criteria interfere in the visual inspection process, such as:

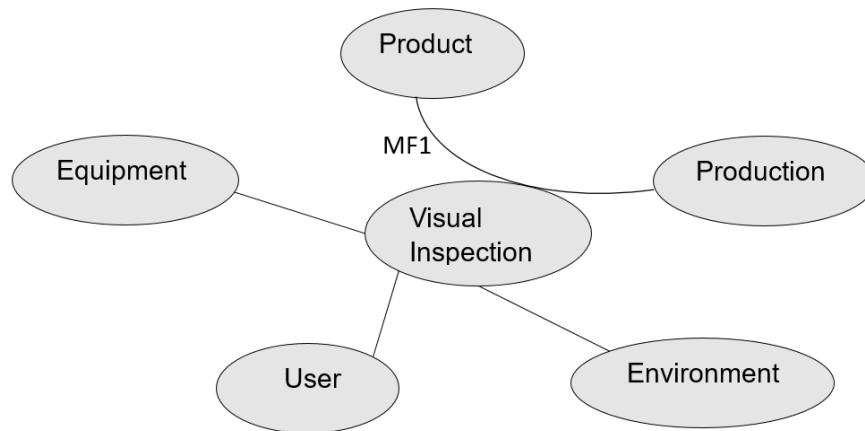


Figure 5.10: Diagram representing the main function (MF1) of visual inspection and its related parameters

1. Equipment: it refers to all the fixtures, technical equipment, computers and machinery used in a plant, *ie.* robot, programmable logic controller and personal computer.
2. User: it is the operator who loads/unloads the product.
3. Environment: it includes all the surroundings or conditions in the plant's area, *ie.* light and dust.

These criteria's correlations may have an impact on the production line in terms of availability, performance and quality. Visual inspection is actually done by the operator, making the reliability highly improvable, as demonstrated in Chapter 4. The goal is to automate the connection between the operator and the visual inspection. The impact of the automation on the reliability in detecting defective parts in the production line will be tracked.

5.2.5/ LEAK TEST

Testing manufactured parts to make sure fluids can't leak into or out of the part is called a leak test. It allows to ensure the proper function and maintenance of industrial systems and pipelines while calculating the loss of pressure. This loss of pressure is measured with an air diffusion that enters from the inlet and then gets out from the outlet. If a pressure loss is detected, a rework should be manually applied by the operator on the concerned welding seam.

5.3/ VISUAL INSPECTION OF WELDING SEAMS IN FAURECIA PLANTS

5.3.1/ REFERENCE PART

Figure 5.11 shows the reference part: it is the cold line sub-assembly of the exhaust system, in which four welding seams need to be inspected. These seams are obtained via MIG and MAG welding.

Confidential

Figure 5.11: Sub-assembly part to be checked

5.3.2/ DATA COLLECTION

The camera installation is shown in Figure 5.12. Implementing artificial intelligence in the plants remains a challenge in today's manufacturing industries [67, 57, 71]. One of the challenges encountered when collecting data from the plant is the defined procedure. We have previously tested a data collection to train the AI model. The operator used to launch manually the image acquisition for every reference part. This data collection has impacted the cycle time of the operator and did not meet the expectations of the plant. For that, data collection of this project was made automatically and took eight months. We have collected around 250 welded reference parts per month and have faced connectivity issues while transferring data outside the plant. Hence, these are some of the constraints linked to the equipment's parameter as listed in Figure 5.10. The camera used is an 18MP device, positioned above the reference part at a distance of 1200mm in order to cover all regions of interest. Figure 5.13 represents the images collected for each reference part. On the left, we can notice the first side of the reference part, containing three welding seams. On the right, we have the remaining fourth welding seam to be inspected.

Confidential

Figure 5.12: The camera installation in a Faurecia plant

Confidential

Figure 5.13: Images collected for each reference part

All images should be cropped so the Artificial Intelligence (AI) model can focus on the different regions of interest. Cropping is performed prior to training the model in order to verify that the defect is still present inside the image even after the image has been resized. Collected images are cropped in four smaller images in order to cover the four different welding seams. Around 80% of the collected data were used for training and 20% for testing. The classification of images is done by the plant and this classification allows the validation of the test dataset once the AI models are created.

5.3.3/ OPERATING PROCEDURE

The welding seam is done by the robot. Once the welding of a specific reference part is finished, the associated information is sent to the Programmable Logic Controller (PLC). A PLC plays an intermediate role between the robot and the Personal Computer (PC). Its aim is to convert hexadecimal data received from the robot to binary data, understandable by the PC, and vice versa. Then, the PLC alerts the PC in order to launch the image acquisition of the reference part. This procedure is repeated each time a new reference part is welded by the robot. After that, the leak test process takes place.

By verifying all welding seams, the quality of the product is guaranteed. Due to their positions, four of these welding seams cannot be verified by the leak test, so operators have to manually inspect their quality. Hence, an automated visual inspection need to be implemented.

5.3.4/ PARAMETERS CONTRIBUTING TO THE QUALITY OF WELDING SEAMS

Confidential

Confidential

Figure 5.14: Representation of alpha and beta angles used in the torch angle parameter

5.4/ DEEP LEARNING SOLUTION FOR AUTOMATED WELDING SEAMS QUALITY CONTROL

In Chapter 3, we presented deep learning architectures able to classify images. One of these architectures is MobileNet. Its depthwise convolution makes that fewer number of parameters and fewer multiplications are used. By that, the model's size and complexity

are reduced. Hence, a MobileNet architecture provides smaller model to predict, which implies less execution time per prediction.

The MobileNet architecture will be applied on the collected dataset.

5.4.1/ DATASET CHALLENGES

Images have been collected in a Faurecia plant, following the operating procedure described in Section 5.3. The distribution of images relative to four welds, each one having five different defects for NOK images, is represented in Table 5.1. It shows that around 2000 OK images were collected per weld, while NOK images varies between 66 and 215 per weld. We can identify an imbalanced dataset in the collected images which makes the model's predictions biased.

Table 5.1: Distribution of collected images for OK and NOK classes

Weld area	OK training	NOK training	OK test	NOK test
Weld1	100	100	1736	44
Weld2	50	50	1944	16
Weld3	90	90	1848	25
Weld4	150	150	1659	65

5.4.2/ DATA AUGMENTATION DEFINITION

The performance of a neural network is directly proportional to the amount and diversity of data available during training. Many techniques can be applied on the images in order to obtain balanced dataset [2, 4, 50, 13]. One of these techniques is data augmentation, which permits better control on the given input to the neural network [50, 13]. Applying data augmentation techniques can be done while training the neural network. It is used to increase the amount of data by adding modified copies of existing data. It helps enlarging the dataset while feeding the neural network with relevant data: data having same properties as the original dataset. By that, overfitting is reduced because the neural network treats these images as distinct images.

In this contribution, the approach is as follows:

1. Adjust the imbalanced dataset (insufficient NOK images) of real reference parts collected from the plant using data augmentation techniques.
2. Test different DL approaches (including the raw dataset) aiming to reach the required precision in detecting defective parts.

5.4.3/ DATA AUGMENTATION FILTERS

In order to obtain better precision when predicting, filters can be applied on the images. Seven of them were tested on weld1 as shown in Figure 5.15. Following is the description of each applied filter:

1. RGB filter: it takes an RGB image as input and splits the three channels before saving each one in a separate image. It is represented in Figure 5.15 by *RGB Filter Red*, *RGB Filter Green* and *RGB Filter Blue*. This filter multiplies the original dataset by four.
2. Mode filter: it is used to remove noise from an image. It selects, inside a fixed-size square window, the most frequently occurring pixel value. Then, it assigns the selected value to all the pixels belonging to the window. The most frequently used kernel sizes are three, five, seven and nine. Figure 5.15 displays the example of *Mode Filter 9*. This filter multiplies the original dataset by five.
3. Box blur filter: each pixel is assigned with the average value of the neighboring pixels inside a squared window. In our training, the size values of the box blur filter vary between four and seven. Figure 5.15 shows only the *Box Blur 7* version. This filter multiplies the original dataset by five.
4. Rank filter: Rank filters uses the local gray-level ordering to compute the filtered value. In our applications, we only use the max, min and median ranks. They are represented in Figure 5.15 by *Rank Filter Max 9*, *Rank Filter Min 9*, and *Rank Filter Median 9*. Each filter is trained alone with rank values equal to three, five, seven and nine. Thereby, the original dataset is multiplied by five for each rank value (Max, Min and Median).
5. Translation: it performs a geometric transformation which changes the position of each pixel inside the input image. Ten different variations were applied vertically, ranging from -5 to $+5$ (Figure 5.15 displays the example of *Translation 5*). Hence, the original dataset is multiplied by eleven.
6. Rotation: a rotation of the original image is applied with an angle equal to 180° . It changes the sense of direction of the welding seam while keeping its geometry (represented in Figure 5.15 by *Rotation 180*). This filter multiplies the original dataset by two.
7. Flip: this mirror effect is done by reversing the pixels horizontally. In this case, the flipped image keeps the shape of the welding seam (represented in Figure 5.15 by *Flip*). This filter multiplies the original dataset by two.



Figure 5.15: Examples of data augmentation techniques applied on weld1

5.5/ IMPLEMENTATION DETAILS

5.5.1/ ANALYSIS OF THE COLLECTED DATA

Based on the collected data, some regions of interest have less than 100 NOK images. For example, we only have a total of 66 NOK images of the weld2 region. 80% of this dataset (around 50 images) has been used for training, only 16 images remained for testing. This number is not sufficient to validate the model.

Merging images from different welds may be a benefit for welds where the number of NOK images is insufficient. This method will allow regions with low number of NOK images (such as weld2), to benefit from regions with sufficient number of NOK images (such as weld4). The detailed results presented in Table 5.2 confirm that better results are obtained with the merged model (weld1-2-3-4) compared to a standard model (weld2).

5.5.2/ CROSS VALIDATION

Cross validation is a resampling technique that allows to ensure that the AI model has learned the data features in a correct way. In other terms, it reduces the impact of noise in its decision making process, guaranteeing its efficiency and accuracy [51, 75, 69]. The model will be able to predict the output correctly when new images are presented as input.

The method used in our case to test cross validation is the holdout method. The collected

Table 5.2: Comparison between different data augmentation filters applied on four welding seams

Weld Number	Data augmentation filter	OK accuracy (%)	NOK accuracy (%)
Weld1	No data augmentation	87	98
Weld1	RGB	98	93
Weld1	Mode	97	95
Weld1	Box blur	97	100
Weld1	Rank	98	97
Weld1	Translation	97	98
Weld1	Rotation	98	93
Weld1	Flip	96	91
Weld2	No data augmentation	53	81
Weld2	RGB	70	93
Weld2	Mode	90	56
Weld2	Box blur	99	75
Weld2	Rank	99	76
Weld2	Translation	87	87
Weld2	Rotation	53	87
Weld2	Flip	15	100
Weld3	No data augmentation	100	16
Weld3	RGB	94	96
Weld3	Mode	100	36
Weld3	Box blur	98	72
Weld3	Rank	99	76
Weld3	Translation	92	84
Weld3	Rotation	93	68
Weld3	Flip	99	32
Weld4	No data augmentation	96	98
Weld4	RGB	99	86
Weld4	Mode	96	97
Weld4	Box blur	98	95
Weld4	Rank	98	93
Weld4	Translation	95	97
Weld4	Rotation	97	91
Weld4	Flip	97	95
Weld1-2-3-4	No data augmentation	96	95
Weld1-2-3-4	RGB	96	95
Weld1-2-3-4	Mode	97	95
Weld1-2-3-4	Box blur	97	95
Weld1-2-3-4	Rank	97	95
Weld1-2-3-4	Translation	94	95
Weld1-2-3-4	Rotation	91	96
Weld1-2-3-4	Flip	88	97

dataset is manually splitted in 3 sub categories: training, validation and testing. This way, the data presented as test data in the first learning phase, will be used as the training data in the second one. If the results of both trainings are close to each other, then the

model got most of the patterns from the data correct.

Table 5.3 shows the results of cross-validation when applied in three different tests on weld4. Having an accuracy of 96% and 98% on the OK and NOK predictions respectively means that the collected model is robust and will reach around the same accuracy once applied on live data.

Table 5.3: Results of cross validation applied on weld4

Index	% OK	% NOK
Cross validation 1	96%	98%
Cross validation 2	94%	100%
Cross validation 3	98%	97%
Average	96%	98%

5.5.3/ EXPERIMENTAL ENVIRONMENT

The experimental environment is powered by Intel i5 CPU, 2.30 GHz with 64-bit, Windows 10 system and 8 GB memory. The software programming environment is Python. It uses Tensorflow as backend. In the image classification model, Root Mean Squared Propagation (RMSProp) is selected as an optimizer of the CNN. The learning rate decay type is exponential starting with a value of 0.01 and ending with a value of 0.0001. The input of the CNN is a 4D array. It has a shape of (batch size, height, width, depth). The batch size defines the number of samples that will be propagated through the network. The other parameters represent the height, width, and depth of the images. In our experiment, the input has the following values (32, 128, 128, 3). The model has been trained with 9000 epochs. Each epoch processes the entire data set through the neural network only once.

5.6/ EXPERIMENTAL RESULTS

Table 5.2 shows the results obtained on the weld1, weld2, weld3 and weld4 welding seams. With weld1, the *box blur* filter bypasses the target and reaches 100% of accuracy on the NOK parts. For weld2 and weld3, the RGB filter provides the best results, with 93% and 96% of accuracy on NOK parts respectively. As for weld4 the target of 97% for NOK parts is reached with several filters (mode and translation filters). The best balance of accuracy between the OK and the NOK parts of weld4 is reached when no data augmentation is applied. This model has been chosen for live tests.

The model where all welds are merged reaches the target with 98% of accuracy on NOK parts when it is trained with the mode filter.

5.7/ CONCLUSION

This contribution proposes a method based on deep learning and image processing to inspect welding seams, the features of the dataset are extracted by MobileNet architecture.

The results show that the target of 97% is reached with the weld1 and weld4 with an accuracy of 100% and 98% on NOK predictions respectively. As for weld2 and weld3 with an accuracy of 93% and 96% respectively, the challenge remains present.

Generative Adversarial Networks (GAN) allow to obtain augmented relevant dataset. This architecture uses two neural networks: a generative model and a discriminative model, competing with each other to become more accurate in their predictions [5].

Besides, One Class (OC) architecture proposes to train the model with one class in order to extract features. Eventually, One Class Convolutional Neural Networks (OC-CNN) apply the OC concept on a standard CNN and have already reached a high precision in detecting intrusions when compared to the trained cluster [14]. In our future work, we plan to apply GANs and OC-CNNs on the welds' dataset in order to reach the defined accuracy's target.

PARAMETERS CORRELATION OF DEEP LEARNING MODEL

6.1/ INTRODUCTION

As presented in Chapter 5, welding is a manufacturing process consisting in joining two or more elements in a permanent way while ensuring continuity between these elements [47]. The assembly is done either by heating, by applying mechanical pressure, or combining both techniques.

In the previous chapter, we applied MobileNet architecture to identify welding defects. The model has been evaluated solely by its accuracy and the percentage of true positive and true negative results it achieves. However, reaching the accuracy target with the AI model prediction may be insufficient to guarantee that the model is accurate.

Model interpretation is becoming a primary evaluation metric as well as its performance [9]. One of the interpretation methods is the heatmap, a visual representation assigning colors to data importance, created by a software algorithm. A compromise between explainability and accuracy is more and more necessary in industrial applications.

The proposed approach in this contribution consists of:

1. Displaying the heatmap of a deep learning model trained with the welding seam dataset.
2. Correlating the heatmap with traditional deep learning classes' scores.
3. Proposing a hybrid approach: integrating machine learning classifiers in order to improve the overall accuracy.

6.2/ PARAMETERS CORRELATION

Causality is an indication of how strongly one variable depends on another (relationship between cause and effect). In deep learning, the accuracy parameter measures how well a trained model is performing.

Displaying the heatmap, relative to an AI model, allow to identify which variable is having a high or low correlation with regard to another variable. In this section, we will first present the heatmap definition and how to interpret it visually. Then, we will discuss the deep learning accuracy calculation and how to improve the model reliability.

6.2.1/ VISUAL EXPLANATION OF THE HEATMAP

The explainability of the AI model reinforces the credibility of the obtained results and allows to evaluate the reliability of the model and its behavior if a partial change occurred in data [78, 36, 24]:

Selvaraju *et al.* [10] have first proposed the Gradient-weighted Class Activation Mapping (Grad-CAM) method, a visualization technique able to tell which parts of a given image led the trained CNN to its final classification decision. This method makes it easy to debug the decision process of a CNN, especially in the case of misclassification. The result of this method is an activation heatmap indicating the parts of the image that have contributed the most to the final decision of the network.

In the same context, Zhang *et al.* [78] have applied such model explainability to interpret the deep learning models trained to classify multiple sclerosis types in the brain using the Grad-CAM method. The experimental results showed that Grad-CAM gives the best heatmap localizing ability, and CNNs with a global average pooling layer and pre-trained weights achieve the best classification performance.

The Grad-Cam method has proven its ability in explaining deep learning model's decision-making. This method will be added to MobileNet architecture aiming at further improving its accuracy.

6.2.2/ DEEP LEARNING ACCURACY CALCULATION

Since weld defects are not always present in production, images corresponding to Not OK (NOK) class occur with a lower probability than images associated to OK class, so this is obviously an imbalanced dataset problem [34].

Welding seam's classification was initially solved by applying data augmentation techniques[56]. A deep learning model based on MobileNet architecture has been trained on a set of images corresponding to four welding seams. Figure 6.1 shows how each welding seam's dataset is classified.

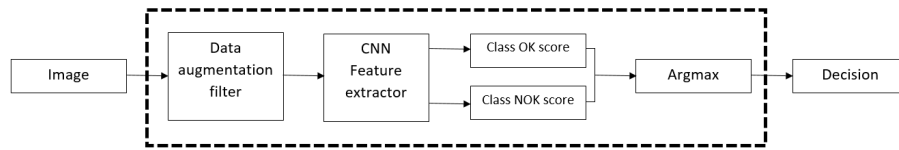


Figure 6.1: Decision-making approach for MobileNet architecture

The proposed solution has reached the client's requirements: 97% of NOK predicted as NOK on weld1 and weld4. We have noticed that the *flip* filter has reached 100% of detected NOK images on weld2. However, its OK accuracy is 15%, making by that the prediction highly improvable and not sufficient as it is. In order to prevent over quality and avoid sending OK reference parts to rework, we will try to find a better compromise between OK and NOK accuracy of weld2.

As for weld3, none of the data augmentation filters has reached the accuracy target of 97% on NOK parts. For that, we have chosen the rotation filter, with 93% and 68% of precision for OK and NOK parts respectively.

The challenge remains present on weld2 and weld3 with an average accuracy value of respectively of 57.5% and 80.5%. Hence the need to look for other methods to overcome this problem. Table 6.1 displays the best accuracy results, obtained when applying data augmentation techniques on MobileNet architecture.

Table 6.1: Best results reached with data augmentation techniques on weld1, weld2, weld3 and weld4

Weld Number	Data augmentation filter	Accuracy
Weld1	Box blur	98.5%
Weld2	Flip	57.5%
Weld3	Rotation	80.5%
Weld4	No data augmentation	96.5%

6.2.3/ MODEL RELIABILITY

Model reliability is considered as an important criterion when choosing the best model [18, 23, 65]. Even if the accuracy target is achieved, the model might use a biased part of images to perform the classification, which causes a drop of accuracy when facing new input data.

Heatmap visualization is a graphical representation of numerical data. It uses matrices where each cell represents the intensity of the studied event. In deep learning, heatmap is used to represent the weights distribution relative to the model's decision-making [85]. Warm colors represent high-value weights in the deep learning model while cool colors

represent low-value weights.

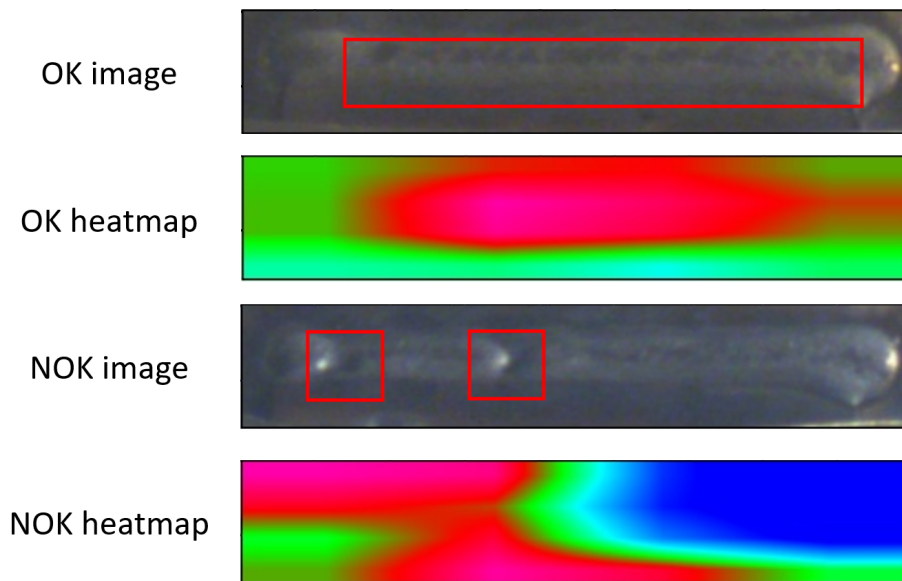


Figure 6.2: Heatmap visualization of OK and NOK weld2 images.

Figure 6.2 shows an example of both OK and NOK images and their relative heatmap visualization. The red square in the OK image represents the zone of interest on which the model should be based on when classifying an OK image. The OK heatmap shows the section on which the model relied on for classification (warm colors sections). The NOK image shows two defects, surrounded by the red squares. As for the NOK heatmap, it shows that the warm colors are not correctly distributed: the warm colors are not superimposed with the zones of interest displayed on the NOK image. This means that the model used a biased decision-making, based on pixels excluded from the zone of interest. Indeed, this NOK image has been misclassified by the model.

Although the model has good overall accuracy on the dataset, it is necessary to study the reliability of the model: in addition to its accuracy, a possible correlation between the activation heatmap results and the model classes' scores can be identified.

6.3/ STATE OF THE ART OF HYBRID METHODS

Ahlawat *et al.* [21] have implemented a hybrid method using CNN and Support Vector Machine (SVM) classifier for handwritten digit recognition: CNN works as an automatic feature extractor and SVM works as a binary classifier. Their results showed that the hybrid approach achieved an accuracy of 99.28% on the Modified National Institute of Standards and Technology (MNIST) dataset.

Soumaya *et al.* [74] have tested a hybrid classification model using a genetic algorithm and SVM to detect Parkinson's disease. Their method attempts to give an accuracy of

80% and 72.50% using two kernels of SVM. The hybrid method seems to ensure the optimization of the classification system by minimizing the dimension of the features vector and maximizing the accuracy.

In the same context, Ahammad *et al.* [20] have suggested a new CNN-deep segmentation-based boosting classifier for spinal cord injury prediction. This method gives 10% improvement on the classification rate.

Another hybrid method is developed by Liu *et al.* [12] for CO₂ welding defects detection by using CNN for primary features extraction and Long Short-Term Memory (LSTM) for feature fusion. The algorithm reaches 94% of prediction accuracy.

Hybrid methods can reach higher accuracy when the right parameters are correlated together.

6.4/ METHODS FOR IMPROVING THE AI MODEL RELIABILITY

6.4.1/ MODEL EXPLAINABILITY

The main approach of this contribution is based on the Grad-CAM method, introduced by Selvaraju *et al.* [10]. This method assigns importance to each weight value in the last convolutional layer by producing a coarse localization map of important regions in images. It computes the linear combination of activations, weighted by the corresponding output weights of the predicted class. The resulting class activation mapping is then resampled to the size of the input image. Grad-CAM allows to ensure that the deep learning model is looking at the correct patterns.

6.4.2/ HEATMAP ANALYSIS

Each pixel of the heatmap is assigned to one of these clusters : *red cluster*, *green cluster* or *blue cluster*. The choice is made based on the channels values of each pixel, the pixel will be assigned to the cluster relative to the channel having the highest value. For example, if a pixel has a color intensity distributed as follows: 128 in the red channel, 181 in the blue channel, 100 in the green channel. Then, this pixel will be added to the blue cluster.

Pixels that belong to the red cluster will be more similar in color, in particular in Red intensity, than pixels belonging to another cluster. Once all of the pixels are distributed on the three clusters, the Red Color Ratio (RCR) of an image can be calculated. Following is the formula applied to get the RCR:

$$RCR = \frac{\text{Number of red cluster pixels}}{\text{Total number of pixels}} \times 100$$

Figure 6.3 shows the distribution of classes' scores related to weld3 images. These scores are the result of the trained AI model with MobileNet architecture presented in Chapter 5. Each blue dot is a defective weld (NOK image), and orange triangles represent non-defective weld in reality (OK image). Defining a threshold in order to separate both clusters is not possible with classes' scores.

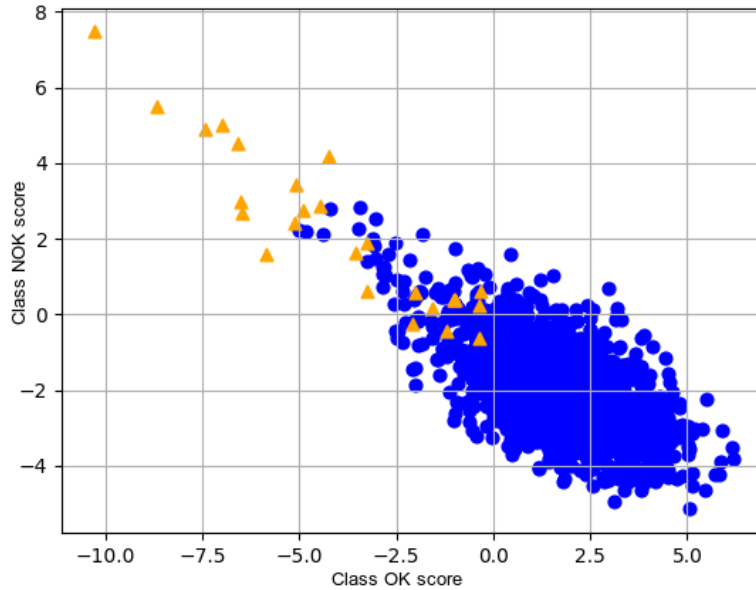


Figure 6.3: Distribution of weld3 images per classes' scores

A better visualization of both clusters is represented in Figure 6.4. It is obtained by correlating the RCR parameter with classes' scores. This correlation offers better visibility on the cluster's distribution, compared to Figure 6.3.

This correlation will be used for the rest of this study. Having numerical input data, a Machine Learning (ML) classifier should be used to assign a class label to these data inputs.

6.4.3/ MACHINE LEARNING CLASSIFIERS

We have tested many ML classifiers to improve the decision-making. Following are the tested ML classifiers:

1. Extreme Gradient Boosting (XG-Boost) classifier: it is a gradient boosting algorithm that offers a panel of hyperparameters. It is possible to have total control over the implementation of Gradient Boosting [6]. During the experiments, this booster is called *gbtree* and uses a tree-based boosting. In our actual experiments, the step

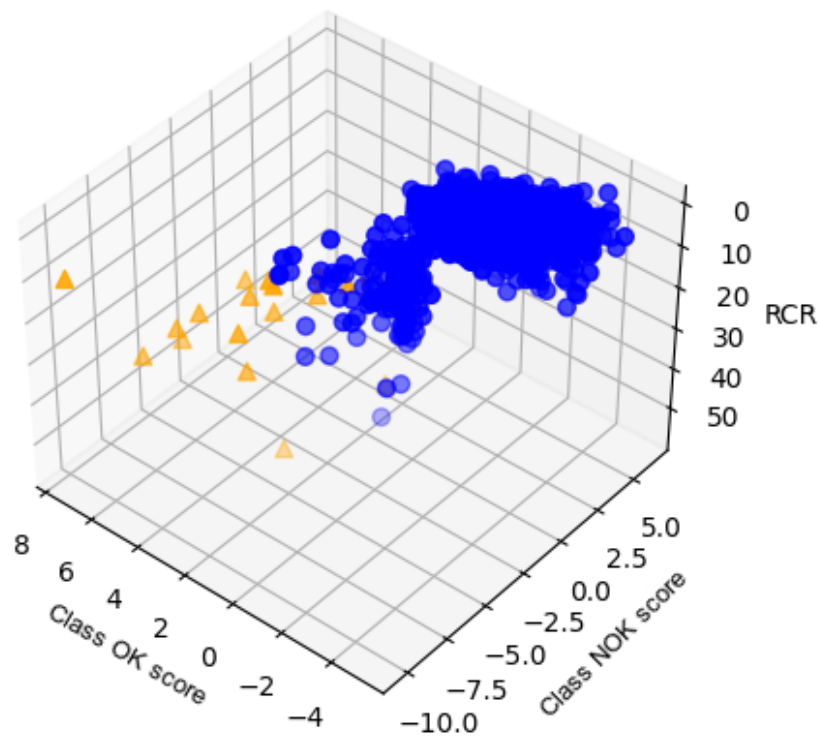


Figure 6.4: Correlating classes' scores with Red Color Ratio for weld3 images

size shrinkage was set to 0.5 and the *uniform selection* was chosen as sampling method.

2. Decision tree classifier: it uses the Gini function to measure the quality of the split. Gini index measures the probability of an observation [87] and identifies the degree of a particular variable being wrongly classified when it is randomly chosen. The max depth is set to the default value so that the tree nodes are expanded until all leaves are pure or contain less than two elements.
3. Support Vector Machine (SVM) classifiers: they are machine learning algorithms that solve classification and regression problems, known for their strong theoretical guarantees and their great flexibility. SVM projects data into a higher-dimensional space and makes them separable. They become a universal approximator [1]: with enough data, such an algorithm can always find the best possible boundary to separate two classes. SVMs uses Kernel functions called SVM kernels, they systematically find Support Vector Classifiers (SVC) in higher dimensions.

In this contribution, two SVM kernels were used:

- Linear Kernel: it is a linear classifier. Data are assumed to be linearly separable using a single line.

- 5-Polynomial Kernel: it has a parameter d that stands for the degree of the polynomial. When $d=1$, the polynomial kernel computes the relationships between each pair of observations in 1-Dimension and these relationships are used to find a SVC. When $d=2$, the Polynomial kernel computes the 2-Dimensional relationships between each pair of observations and those relationships are used to find a SVC. The polynomial degree applied in our tests, is equal to five.

Adding a machine learning classifier changed the way each welding seam has been classified (previously presented in Figure 6.1). This solution offers a classification scheme as presented in Figure 6.5.

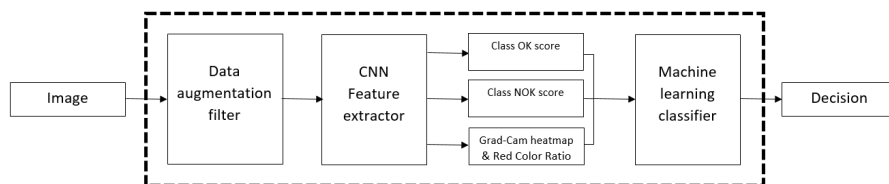


Figure 6.5: Proposed decision-making approach: adding Grad-CAM heatmap and Red Color Ratio

6.5/ IMPLEMENTATION DETAILS

6.5.1/ DATA COLLECTION

The dataset we used in [55] has been collected in order to improve the accuracy in detecting defective parts, which the client wanted above 97%. However, the target was not reached on weld2 and weld3 with our previous experiments. Many data augmentation filters have been applied on these two welds and one specific dataset has been chosen for each of these welds, based on the potential improvement of their associated accuracy, as below:

1. Flip filter has been selected for weld2: previously reached 15% on OK images and 100% on NOK images (an average of 57.5%).
2. Rotation filter has been selected for weld3: previously reached 93% on OK images and 68% on NOK images (an average of 80.5%).

6.5.2/ EXPERIMENTAL ENVIRONMENT

The experimental environment was powered by one Intel i5 CPU, 2.30 GHz with 64-bit, Windows 10 system and 8 GB memory. The software programming environment is Python. It used both Keras and Tensorflow as backends. RMSProp was selected as the optimizer of the MobileNet model. The chosen learning rate decay type was exponential starting with a value of 0.01 and ending with a value equal to 0.0001. The model has been trained with 9000 epochs.

6.6/ EXPERIMENTAL RESULTS

Four of the machine learning classifiers have been applied following the proposed approach. As detailed in Table 6.2, weld2's accuracy was improved by +41.8% with XG-Boost classifier. While weld3's accuracy was improved by +18.2% with XG-Boost and SVM 5-Polynomial classifiers.

Table 6.2: Proposed decision making results when applied on weld2 and weld3

Welding Seams	Accuracy per Classifier			
	XG-Boost	Decision Tree	SVM Linear	SVM Poly5
Weld2	99.3%	98.1%	98.8%	98.8%
Weld3	98.7%	97.2%	98.1%	98.7%

These results prove that adding a statistical machine learning classifier after the feature extractor and class activation heatmap does increase the overall accuracy of the model for both welds. The target accuracy is reached, with a tiny advantage to XG-boost classifier.

6.7/ CONCLUSION

In this contribution, a hybrid approach of CNN-Machine Learning Classifier is proposed for welds defects classification. This approach adds a new reliability score calculated using the Grad-CAM heatmap.

The hybrid approach proposed reaches high accuracy on weld defects classification. The highest accuracy improvement was by +72.7% for weld2 using MobileNet-XG-Boost classifier and by +22.6% for weld3 using MobileNet-SVM Poly5 Kernel or MobileNet-XG-Boost classifier. The target defined by the plant's team of 97% detection of NOK parts is now reached and we were able to get rid of the over quality.

This work presents new model-driven optimization methods to improve the accuracy of

vision systems. In future work, this approach can be applied on other deep learning architectures to validate its efficiency.

BRICK ORIENTATION ADJUSTMENT USING IMAGE PROCESSING TECHNIQUES

7.1/ INTRODUCTION

Ceramic monoliths sit right in the center of exhaust pipes and transform dangerous gases from the engine into harmless gases. They act as a filter. Quality control has already been applied, at filter level, to measure the distribution of particles [3]. Quality control should also cover the performance of soot combustion in ceramic monoliths [32] and particle filtration, based on the theory of the packed bed of spherical particles [43].

Faurecia is working on guaranteeing the quality of their productions. For this purpose, one supplementary parameter that needs to be controlled was identified: the angular position of the ceramic during the assembly step. It needs to reach a 99% level of accuracy with a tolerance of ± 5 degrees. This quality control also needs to be automated and implemented in an accurate and repeatable system. Moreover, in order to interact promptly with the operator, the automated control algorithm should run in less than 0.8 seconds. In this chapter, the approach will be the following:

1. Listing the related works to detect straight lines.
2. Diving into image processing techniques to detect straight lines of ceramic monoliths.
3. Comparing between different image processing techniques, and validating the chosen technique with a repeatability test.

7.2/ PROBLEM STATEMENT

7.2.1/ STUFFING TECHNIQUE

Ceramic monoliths sit right in the center of exhaust pipes and transform dangerous gases from the engine into harmless gases. These gases are born from the combination of precious metals such as Platinum, Palladium and Rhodium. An example of a ceramic monolith is represented in Figure 7.1. **Confidential**

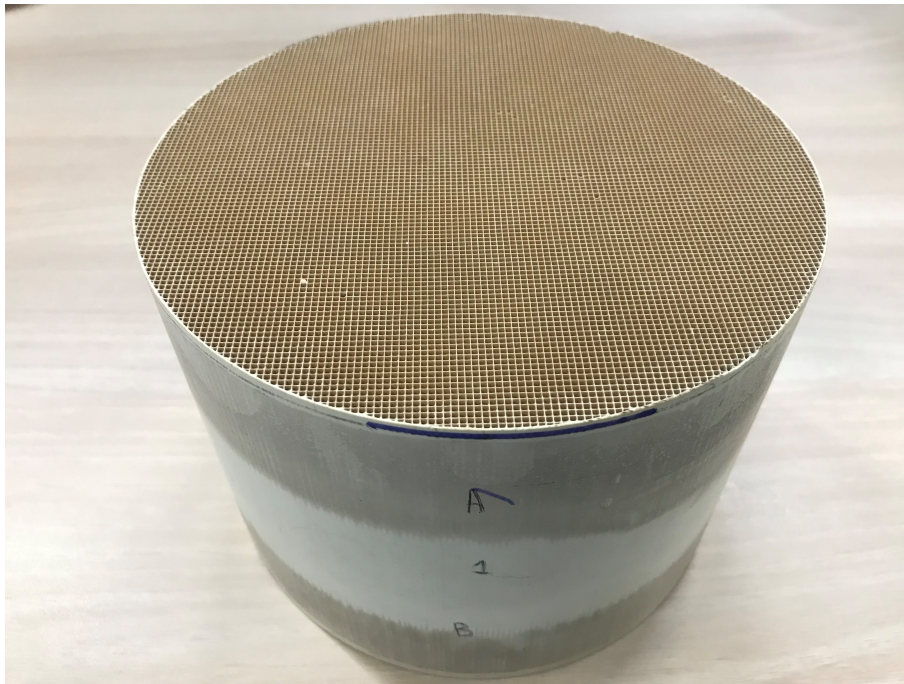


Figure 7.1: Example of a ceramic monolith

Confidential

Figure 7.2: Stuffing technique

7.2.2/ RISK OF BREAKAGE

The orientation of the ceramic monoliths does not affect the filtration of engine exhaust gases, but a bad angle increases the risk of breakage during the production of the exhaust systems: in particular, during the welding process that comes right after the stuffing technique.

To avoid too many breakages, we proposed to adjust, when needed, the orientation of the brick before starting the production. The ceramic monolith would be positioned manually by the operator and the automated control process will display whether the angular position is OK or NOT OK with no delay.

The orientation of the brick can be adjusted once the direction of brick's channels (its straight lines) is detected.

7.2.3/ DEEP LEARNING VS. IMAGE PROCESSING

Detection of straight lines can be achieved through two main approaches: image processing and deep learning [59, 73, 58, 52, 68, 60, 66]. According to the state of the art listed in Chapter 3, some parameters to take into consideration when making a decision such as the time for setup. For example, a deep learning solution can not be integrated in the plants conditions within one day, this is due to the number of images to be collected for the training. In addition, the training cannot be prepared in advance because lighting conditions are relative to the experimental environment. Due to the impact of deep learning on the time to market parameter, the image processing approach will be tested on this brick orientation adjustment.

7.2.4/ ANGLE ANALYSIS

Thanks to the particular mesh of the brick, symmetry is obtained respectively with vertical and horizontal directions. These symmetries reduce the number of possible angles from $[0;360]$ to a range of $[0;90]$.

The tolerance defined by the plant is ± 5 degrees. Therefore, the calculated angle has to be in the range $[real_angle - 5^\circ; real_angle + 5^\circ]$.

Moreover, since the channels of the brick have two perpendicular directions and that the detection of one direction or the other does not pose any constraint, this allows us to deduce that an angle equal to 0 degree in real can be detected by the algorithm as a 90 degrees angle. If a real angle is equal to 35, the algorithm can detect it as a 35 degrees or a 55 degrees with a tolerance of ± 5 degrees.

As presented in the image processing's state of the art in Chapter 3, the methods to be tested for highlighting edges are the Canny filter and the Laplacian detector.

7.3/ IMAGE PROCESSING METHODS FOR ANGULAR POSITION MEASUREMENT

In this section, two steps need to be differentiated: firstly, the highlighting of the edges and secondly the straight lines detection. The highlighting of the edges is a preparation step before the straight lines detection. The Canny and Laplacian filters will be tested for edges' highlighting, Hough transformation will be used for straight lines detection.

7.3.1/ HIGHLIGHTING EDGES

CANNY FILTER

The Canny filter method allows to smooth an image and transform it into a binary image [81]. Two parameters are used to smooth an image: the minimum threshold and the maximum threshold allow to determine the desired edge using the gradient formula.

When applying this image processing technique, a pixel belongs to the searched edge if:

1. The pixel gradient is greater than the max threshold.
2. The pixel gradient is between the min threshold and the max threshold and is related to a pixel belonging to the edge.

A pixel does not belong to the searched edge if:

1. The pixel gradient is below the minimum threshold.
2. The pixel gradient is between the min threshold and the max threshold and is not linked to a pixel belonging to the edge.

LAPLACIAN EDGES DETECTOR

The Laplacian is a mathematical function that acts on each dimension of an image (x or y) [81]. It retrieves the evolution of the pixels of each dimension to apply a second derivative. The first derivative makes it possible to know the position of the most accentuated pixels and thus to be able to trace the contours of the images.

The second derivative has the same objective but also eliminates residual noises from the image. Once the function has been re-derived, the only points of interest are the points where the curve vanishes.

7.3.2/ HOUGH LINES

Hough lines allow to detect straight lines in an image. This detection is done either with the polar coordinate system or with the cartesian coordinate system. In this study, the OpenCV implementation is applied; it relies on the polar coordinate system [80].

In this function, a track of the intersection between the curves of every point in the image is kept. The threshold defines the number of intersections needed in order to declare it as a line. This line has θ and $r\theta$ as parameters of the intersection point.

The impact of the methods listed above is represented in Figure 7.3. The original image is displayed on the left, we overlaid in the middle of Figure 7.3 the Canny+Hough result with the original image. On the right is displayed the Laplacian + Hough result overlaid with the original image. The yellow line represents the straight line detected by the algorithm the dotted line (in white) represents the vertical direction that serves as the reference direction. The alpha angle is the angle to be adjusted.

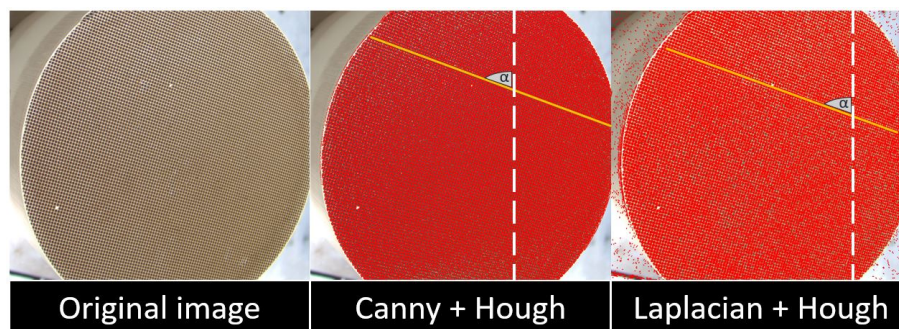


Figure 7.3: Image processing methods applied on the ceramic monolith

7.4/ IMPLEMENTATION DETAILS

7.4.1/ EXPERIMENTAL ENVIRONMENT

The experimental environment is powered by an Intel i5, 2.30 GHz processor with 64-bit on Windows 10 and 8 GB of RAM. The software programming environment is Python. As for the acquisition of images, a Basler acA2500-14gc camera equipped with a FUJINON HF8XA-5M C-mount has been installed (as shown in Figure 7.4). In the plant conditions, the canning machine has a cylinder above, this is why the camera is at twenty five degrees from the vertical direction of the ceramic monolith in the realized tests.

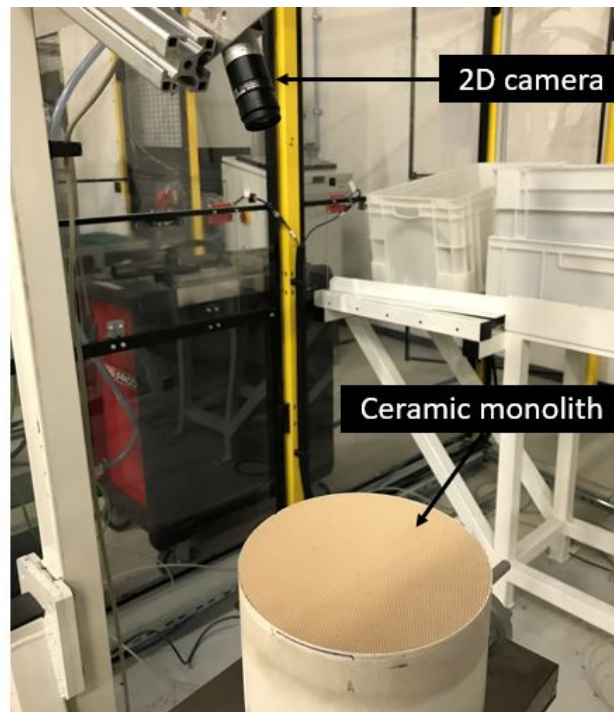


Figure 7.4: Experimental environment: installation of the Basler camera

7.4.2/ IMAGES COLLECTION

Images were collected as in the environment of Figure 7.4. The algorithm automatically collects images of the ceramic monolith with the fixed camera. A step of five degrees is applied on a range from zero to ninety degrees. Thereby, both methods (Hough and Laplacian) are tested on different angles.

The dataset used in this contribution is available here: brick dataset [79].

7.4.3/ VISION PARAMETERS

In order to determine the most appropriate camera's configuration, many vision parameters have been tested to get a clear view of the brick channels (straight lines of the ceramic monolith) [86]:

1. The gain parameter has been tested with different values, as shown in Figure 7.5, from left to right: 0 , 30 , and 60 . It represents the electronic amplification of the signal. A gain increase results in a more brightening image and negatively impacts the quality. We chose to add no gain and to keep the associated value to the minimum (0).
2. The exposure time parameter, represented in Figure 7.6, has been tested with different values, from left to right: 0.12 , 0.48 , and 0.80 .

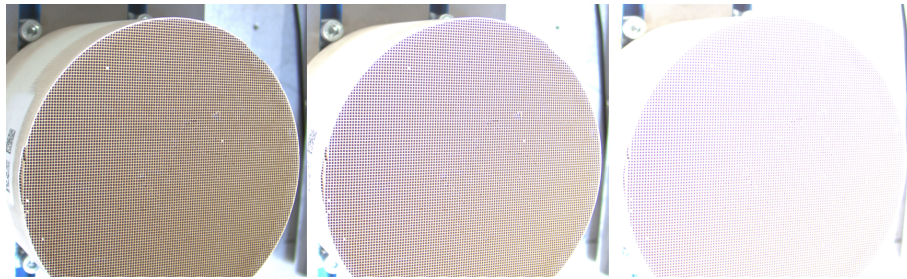


Figure 7.5: Gain: 0 on the left, 30 in the middle and 60 on the right

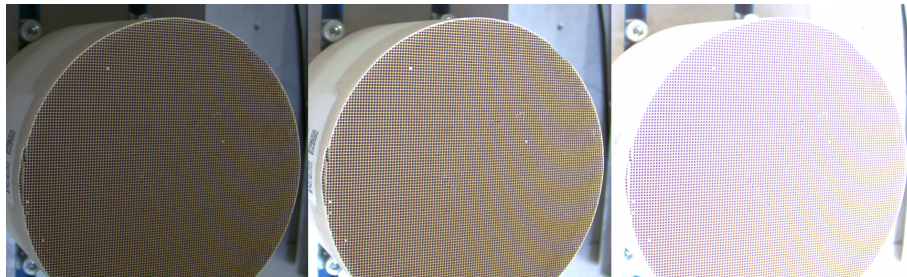


Figure 7.6: Exposure time: 0.12 on the left, 0.48 in the middle and 0.80 on the right

It is the time during which the sensor of the shooting device retrieves information from the image. It depends on the brightness and the aperture of the camera lens. If the exposure time is too low, the sensor cannot recover the pixel values and, as a result, the image is black. Conversely, if the exposure time is too high the image is white. For this project, the exposure time was set to 0.48s.

3. The aperture range parameter, represented in Figure 7.7, is related to the size of the aperture of the camera's mount. The larger the aperture, the more light comes in, the more information the sensor can collect, resulting in a brighter photo. f represents the focal length of the lens divided by the diameter of the aperture opening. In this project, the value chosen for the aperture is equal to $f / 4$.

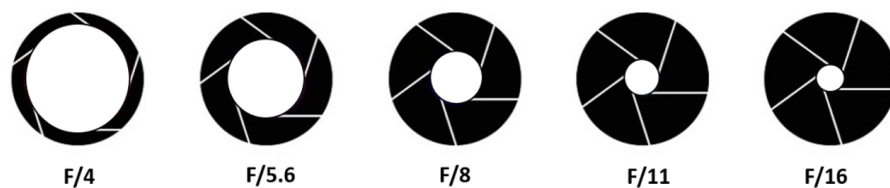


Figure 7.7: Possible aperture values

These parameters have been adapted in order to reach the best visibility of the brick channels and applied on the collected images.

7.5/ EXPERIMENTAL RESULTS

7.5.1/ COEFFICIENT OF DETERMINATION

R-squared (R^2), called coefficient of determination, is a way of measuring how well the regression line approximates the actual data. It is an important indicator of how well the model will interact with future outcomes. The formula of coefficient of determination is as follows:

$$R^2 = \frac{RSS}{TSS}$$

where RSS is the sum of squares residuals and TSS is the total sum of squares.

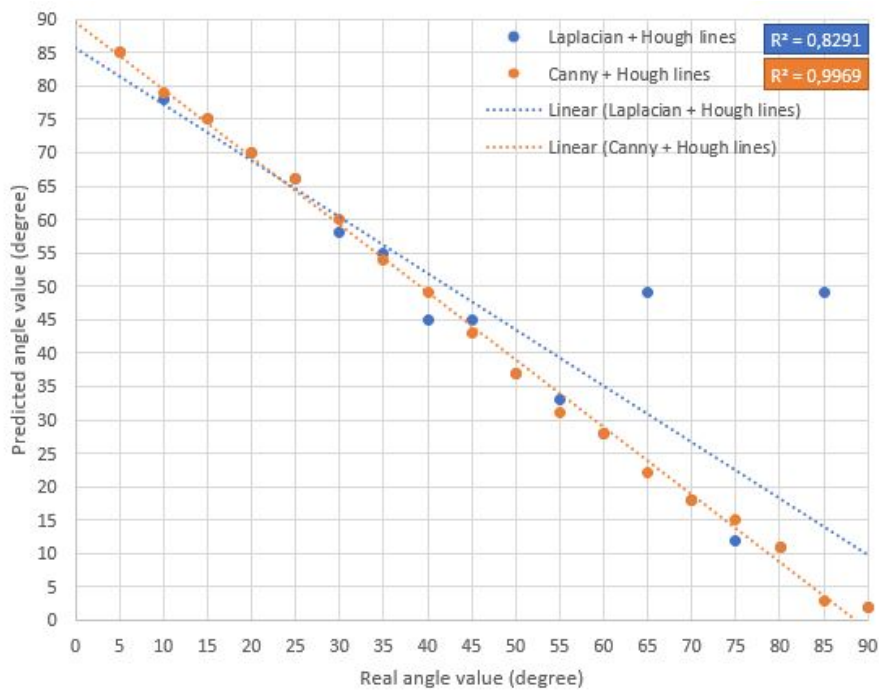


Figure 7.8: Results of Canny-Hough and Laplacian-Hough with linear regression

The results of Figure 7.8 show that:

1. 83% of the predicted angle values with Laplacian + Hough method fit with the real angle values.
2. 99.7% of the predicted angle values with Canny + Hough method fit with the real angle values.

Thereby, the Canny + Hough method bypasses the accuracy required by the plant(99%) with a tolerance of ± 5 degrees. The algorithm execution is 0.6 seconds per image.

7.5.2/ REPEATABILITY TEST

A repeatability test is applied on this method to validate its efficiency. In this repeatability test, the ceramic monolith is fixed, and thousands of images are launched automatically to validate the accuracy of the algorithm through light changes. The first position is at 0 degree, while the last position is at 90 degrees. A step of five degrees is applied.



Figure 7.9: Repeatability test validated with Canny-Hough method

The results of Figure 7.9 show that good detection has a percentage varying between 98% and 100% with an overall average of 99.826%. The algorithm execution of 0.6 seconds is also validated in this test. The Canny-Hough method is now ready to be deployed.

7.6/ CONCLUSION

Quality control of brick channels being executed manually remains not optimal. The automation of such control needs to be done via an algorithm deployed within a cell, offering complete autonomy to the factory.

In this contribution, the orientation of the ceramic is questioned and is addressed by the means of image processing techniques. Similar methods, previously applied for traffic lanes detection [39], have now been validated on the brick channels detection. Tests were carried out by applying a rotation of the ceramic by five degrees. The results show that with the Canny-Hough method, an accuracy of 99.826% is achieved within a tolerance of ± 5 degrees, as requested by the plant.

The proposed solution will be deployed in a Faurecia factory in order to validate the algorithm under real lighting conditions. This deployment will be carried out by the Digital

Expertise & Development team. A Human Machine Interface is still to be designed.

TOWARDS AUTONOMOUS PLANTS: DEVELOPMENT AND DEPLOYMENT OF DIGITAL SOLUTIONS IN THE AUTOMOTIVE INDUSTRY

8.1/ INTRODUCTION

For an innovation to be accepted in manufacturing, it is necessary to have an understandable result, no additional time on the plant's cycle, and a real added value. In the previous chapters, we presented the added value of integrating deep learning and image processing in quality control's automation. In this chapter, we will focus on the Human Machine Interface (HMI) to be installed in the plants. This HMI has been developed by the Digital Expertise and Development (DE&D) team and aims at providing a Plug & Play system to the plants team . It plays an intermediate role between the plant's team and the automated system, by that it enables non-developers to interact with its user interface. In this chapter, we will present the software development context and the industrial context of the HMI, covering different types of quality control. Finally, we will detail the added value of the DE&D digital solution, once deployed in Faurecia's plants.

8.2/ PROBLEM STATEMENT

8.2.1/ FEATURES REQUIRED IN PLANTS

As presented in the state-of-the-art of existing solutions in the market for automatic quality control, following criteria are not covered:

1. re-usable application: to be able to use the same solution for different applications. The software's architecture remains the same, the only difference is the automated type of quality control *ie.* component presence control, welding seam classification, or brick orientation adjustment.
2. remote access: the plant receives the application's hardware and is then able to install the application following the documentation. Remote support for the plant is possible and takes into consideration the network architecture at Faurecia.

8.2.2/ NETWORK ARCHITECTURE

Confidential

Confidential

Figure 8.1: Network architecture

8.2.3/ CYCLE TIME OF A TURNTABLE

Confidential

8.3/ SOFTWARE DEVELOPMENT CONTEXT

It consists in defining the work methodology to be implemented, as well as the development stages to be followed and the HMI architecture.

Confidential

Figure 8.2: Loading/Unloading side of a turntable in a Faurecia plant

Confidential

Figure 8.3: Cycle time of a turntable

8.3.1/ AGILE METHODOLOGY

In this section, we will define the agile methodology implemented in the development of this project. Additionally, we will present the agile terminologies and roles.

AGILE DEFINITION

Agile is a methodology that values a pragmatic mindset and a flexible approach. This methodological framework breaks the project into several phases. It consists on continuously delivering results to clients in an iterative approach. This way, team members can quickly adapt to requirement changes while delivering the highest quality product and increasing customer satisfaction.

Confidential

Figure 8.4: Welding side of a turntable in a Faurecia plant

The DE&D team working on the HMI project is composed of eight members: two Ph.D students, two vision engineers, one roboticist, one automation engineer, one manufacturing project leader and one team manager. The author of this thesis occupies the position of a product owner, an agile role that will be defined later in this section.

AGILE TERMINOLOGIES

Some terminologies are often used in an agile project, following are their definitions:

1. User story: it describes the user experience using the user's language, vocabulary and terminology. For example, a name that succinctly describes the function of the product, the importance that defines the priority of the story, an estimate of the work required and a demonstration. A simple test of the story that will need to be validated and the notes include all the information needed to complete the story.
2. Product backlog: it is the requirements generated from user stories. It represents a mirror of what needs to be done to fulfill the customer's needs and deliver the user story. For example, creating the interface of an application and adding functionality. This product backlog will constantly evolve to reflect new customer needs. Once this product backlog is validated, the realization of the project starts and will be split into several iterations, called *sprints*.
3. Sprint: it begins with a *sprint planning meeting*. Then, during the sprint session, the priority elements in the product backlog will be identified and developed. Each sprint lasts from two to four weeks and includes several steps: development, quality control (validation test), and a delivery. All the deliveries of the cumulative sprints are called the *backlog sprint*.

At the end of each sprint, another meeting will be organized: a *sprint meeting review*. It's about showing the solution through a demonstration, and getting feedback from the client. Any suggested improvement and encountered problems will then be broken down in the product backlog and prioritized in the next sprints.

4. Scrum: it is a meeting are organized on a daily basis during the sprints. It lasts only fifteen minutes and takes place at the beginning of the day. The scrum allows the team to measure the progress of the project and ensure the quality of deliverables and the respect of deadlines.

AGILE ROLES

Now that we have defined agile terminologies, we can identify common routine roles implemented in an agile environment. These roles are listed as follows:

1. Scrum master: ensures good communication between team members identifies organizational obstacles and works to remove those obstacles.
2. Team members: are the ones that are taking the understanding of the project vision and defining what needs to be done for implementation.
3. Product owner: defines the functional specifications and establishes the list of priorities to be developed. This agile actor validates functionalities and user stories with the team members, defines sprints with the client, prepares the product backlogs and organizes the scrum meetings. Additionally, in this HMI development, the product owner proposes Unified Modeling Language (UML) diagrams of the application.

8.3.2/ HMI DEVELOPMENT

Confidential

DEFINITION OF NEED

Confidential

MOCKUP DEFINITION

A mockup is a conceptual tool used to communicate the structure of an application's design by representing detailed design elements. It allows to convert ideas and concepts

Confidential

Figure 8.5: HMI development steps

into a actual design.

Figure 8.6 represents an example of a mockup, designed for the setup module.

Confidential

Figure 8.6: mockup representing the HMI management of a reference part

ACTIVITY DIAGRAM

It graphically represents the behavior of a method or the flow of a use case [88]. An activity represents an execution of a mechanism, a succession of sequential steps. An action corresponds to a treatment which modifies the state of the system. One or more actions form an activity. The sequence of actions constitutes the flow of control.

Different types of nodes are presented in this diagram (bifurcation node, junction node, test-decision node). The work done in this project focused on the test-decision node, rep-

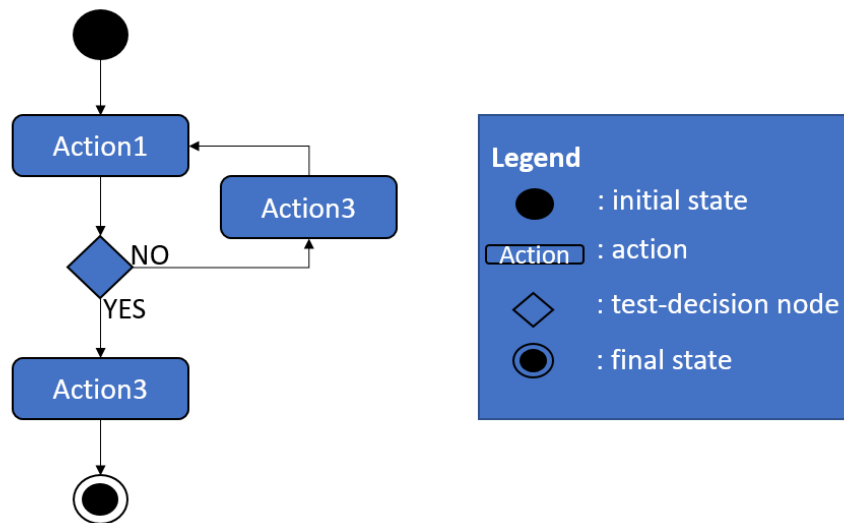


Figure 8.7: activity diagram example representing the test-decision node

resented in Figure 8.7. The test-decision node makes a choice between several outgoing flows according to the guard conditions of each flow. A test-decision node has only one input flow. Two output streams are allowed:

1. the first one corresponding to the condition checked,
2. the second one dealing with the case otherwise [if-else].

SEQUENCE DIAGRAM

An example of a sequence diagram is displayed in Figure 8.8. It represents the interactions between objects by indicating the chronology of the message exchanges [88]. A sequence diagram describes the behavior of objects in one single scenario. It shows objects and messages transmitted between these objects.

A lifeline represents all the operations performed by an object. It shows the period of time during which the object *exists*. Objects communicate by exchanging messages. The vertical dimension represents the flow of time.

CLASS DIAGRAM

A class diagram describes the static structure of the essential entities in the system to be implemented [88]. It is based on:

1. The concept of object: implementing real-world entities.

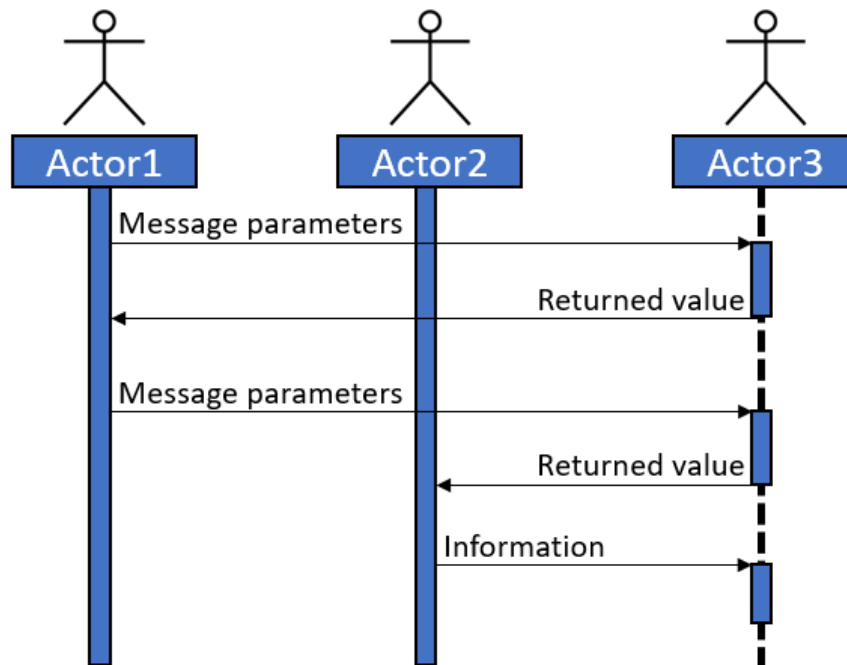


Figure 8.8: communication between actors in a sequence diagram (arrows representing messages)

2. The concept of class: a class can be defined as a data field that has unique attributes and behavior (methods).
3. Different types of association between classes such as composition and aggregation.

The class diagram manages the visibility of attributes and operations, the notion of multiplicity, as well as the relations of composition and aggregation. Figure 8.9 is an example of a class diagram.

A simple association between two classes represents a structural relation between peers, *ie.* between two classes of the same conceptual level. Neither of the two is more important than the other. The multiplicity indicates a domain of values used to specify the number of instances of a class regarding another class for a given association.

An *aggregation* represents a structural link between a class and one or more other classes. It is used to model a relationship between a larger element and a smaller element.

A *composition* is an aggregation relationship in which there is a lifetime constraint between the *component* class and the *compound* class.

A *link* is a physical or conceptual connection between instances of classes and therefore between objects.

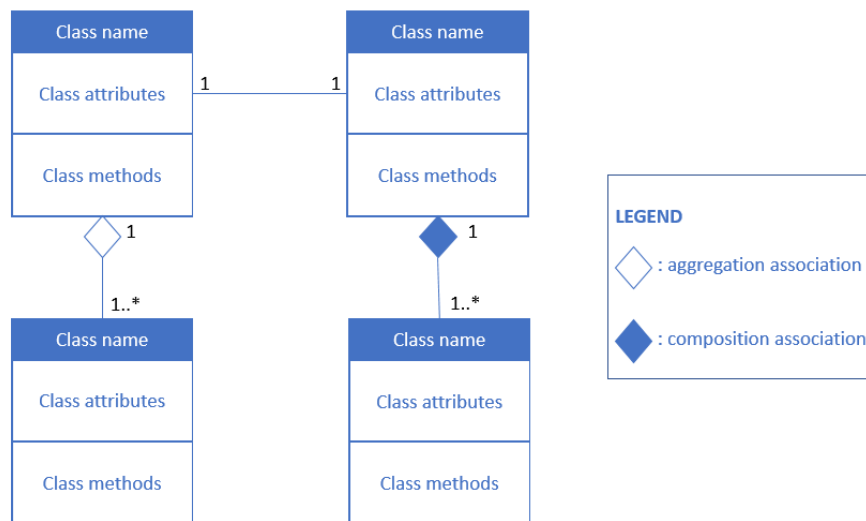


Figure 8.9: Representation of class diagram's elements

VALIDATION TEST

Confidential

8.3.3/ HMI ARCHITECTURE

Confidential

Now that we have discussed the software development context, in the next section we will be talking about the industrial context.

8.4/ INDUSTRIAL CONTEXT

Confidential

Figure 8.10 represents the software computations to be integrated.

Confidential

8.4.1/ INNOVATION PROGRAM MANAGEMENT SYSTEM (IPMS) STEPS

The IPMS is the procedure to be followed in order to deploy an innovative project in Fau-recia plants. This procedure starts with an idea of a project until the project deployment, passing by all of the development phases.

According to Figure 8.11, following are the different phases of the IPMS procedure: *Experiment*, *Concept*, *Feasibility*, *Validation*, *Development*, *Standardization*, and *Deploy-*

Confidential

Figure 8.10: Integrating deep learning and image processing at a hidden time in the cycle of a turntable

ment.

Confidential

Figure 8.11: Steps of Innovation Program Management System (IPMS)

Confidential

8.4.2/ RELEASE PHASES

Facts and data should be presented to go to the next step, through a defense in front of a jury (the steering committee).

RELEASE OUTCOMES

Confidential

STEERING COMMITTEE MEMBERS

Confidential

RELEASE TARGET TIME

Confidential

8.5/ ADDED VALUE OF THE PROPOSED SOLUTION

Confidential

8.6/ CONCLUSION

In this chapter, the digital solution to be deployed in Faurecia plants is presented. This solution allows operators to access the whole automated quality control process from an HMI. The setup is also provided by this HMI: software administrators are able to create, modify or delete reference parts and can define region of interests of any specific connected camera. The software architecture is distributed over modules, which are being deployed progressively in plants by the DE&D team.

A Plug & Play system will be provided to the plants and all the logs will be sent into the private cloud for analysis purposes. These results will then be analyzed in order to further improve the overall quality by identifying correlations among the various parameters.

IV

CONCLUSION & PERSPECTIVES

CONCLUSION & PERSPECTIVES

9.1/ CONCLUSION

In this thesis, automated quality control for component presence control as well as for welding seam classification and brick orientation adjustment have been proposed in order to reduce non-conformities in the automotive industry. In the first part, we have presented the applications of an automated quality control and have covered the scientific background of deep learning, whereas in the second part we have detailed our contributions in this field.

We first presented the product life cycle at Faurecia plants, the need to automate processes in the industry and the existing solutions for this automation in the market. Then, we discussed the state of the art of computer vision techniques: machine learning, deep learning and convolutional neural networks.

In the second part of this dissertation, we detailed our contributions, beginning with the automation of the component presence control, where our proposed solution reached a 100% accuracy on real-life images, collected in the plant's environment. This automation reduces the cycle time by replacing the human visual inspection by an automatic system, delivering high quality results in an optimized time.

The next research work focused on classifying welding seams, by the means of an automated visual control of their external appearance. A weld defect detection rate of over 97% was targeted by the client. The challenge encountered was linked to the imbalanced dataset collected from the plant. To overcome this limitation, we benchmarked many data augmentation techniques in combination with several neural network architectures. Out of the four welding seams to control, we have been able to achieve the minimum defect detection rate on two welding seams while for the remaining two, more data would have been needed.

Nevertheless, to improve the welding bead classification performance detailed above, we then proposed a complementary hybrid approach: combining the visual heatmap results

with the neural network architecture and adding a pre-trained CNN-Machine Learning Classifier. This hybrid solution allowed to achieve the targeted detection rate on all of the four welding seams.

The last research focused on the quality control when assembling ceramic monoliths: positioned at a wrong angle may cause breakages in them. We created an image capture setup, which allowed us to take one picture of the brick before the canning stage. A Canny edge detection filter, followed by a Hough transformation allowed to compute the orientation of the brick with a tolerance of five degrees. The estimated angle value is then displayed to the operator, in order to adjust the brick orientation accordingly.

In this thesis, special attention was given to the integration of deep learning algorithms in the production line and we presented our approach towards providing a Human Machine Interface to the plants. We designed and developed a whole HMI software, in a modular way, ready to run current or future quality control applications. The project has been deployed following the rigorous internal *Innovation Program Management System* procedures and is currently running in Faurecia's plants.

We believe that the solutions proposed in this thesis for various challenges in the automotive industry's quality control can serve as additional and efficient solution choices or tools to address the above-mentioned challenges in automating industrial processes.

9.2/ PERSPECTIVES

There are many perspectives to propose when the work environment is in continuous improvement. The key focus of this thesis was to suggest solutions for automating different types of quality control. The applied solutions are part of deep learning and image processing techniques. One of the main challenges encountered with data collection is that the proposed solutions require thousands of images to be collected. This challenge remains difficult especially when the collected dataset is imbalanced: the number of NOK images is much smaller than the number of OK images. Thereby, one of the approaches to be considered for future researches is to apply Generative Adversarial Networks (GAN) for data augmentation: generating a relevant dataset virtually. By that, the reduction of the needed time to obtain an accurate solution with a traditional deep learning method will result in deploying digital solutions faster.

By definition, GANs are generative modeling approaches that use deep learning methods [7] to automatically discover and learn regularities or patterns from the input data. The model can then be used to generate new examples that could plausibly have been drawn from the whole original data.

GANs are defined as iterative games played between a generator and a discriminator. A

generator is a neural network that generates new instances of data, while the discriminator evaluates its authenticity. The main goal of the generator is to improve its ability in converting random noise into fake data while the discriminator aims at improving its ability in differentiating real data from fake data.

As already stated, the quality control has to be automated in today's manufacturing industry. The work presented in this thesis focused on the integration of the algorithm into the cycle time, but the framework suffers a common weakness: the time to market, *ie.* the time elapsed between the conception of a product and its availability for sale. GANs have the potential to increase the amount of relevant data and to generate realistic defected images. By that, the challenge of the imbalanced dataset could be solved.

Moreover, One Class Classification (OCC) is a type of deep learning algorithms able to detect abnormal data points (outliers) compared to the instances of the known class. These algorithms can solve the problem of imbalanced dataset, in particular the welding seam type of quality control presented in this thesis.

Furthermore, transformers usually applied for natural language processing have been very effective when applied in computer vision, called vision transformers. This deep learning model is based on the attention mechanism. It computes relationships among pixels in various small sections of the image. These sections are then arranged into a linear sequence which creates a series of positional embedding patches. In the end, they are fed to the encoder: a machine learning model that describes an image with a sentence. Vision transformers can be applied in an image classification scenario such as the classification used for quality control in the automotive industry.

Finally, the work done in this thesis opens up limitless perspectives in various research lines. One of the future works is to study applications that can combine different types of quality control in a single deep learning model and to be able to generate automatically relevant features corresponding to the plants environment.

PUBLICATIONS

CONFERENCE PAPERS

- Charbel El Hachem, Gilles Perrot, Loïc Painvin and Raphaël Couturier. *"Automation of Quality Control in the Automotive Industry Using Deep Learning Algorithms"*. In **2021 International Conference on Computer, Control and Robotics (ICCCR)**.
- Charbel El Hachem, Gilles Perrot, Loïc Painvin, Jean-Baptiste Ernst-Desmulier and Raphaël Couturier. *"Welding Seam Classification in the Automotive Industry using Deep Learning Algorithms"*. In **2021 IEEE International Conference on Industry 4.0, Artificial Intelligence, and Communications Technology (IAICT)**.
- Charbel El Hachem, Anass El Houd, Loïc Painvin, Gilles Perrot and Raphaël Couturier. *"Parameters Correlation of Deep Learning Model for Visual Inspection in the Automotive Industry"*. In **2022 International Conference on Computer, Control and Robotics (ICCCR)**.
- Charbel El Hachem, Raoul Santiago, Loïc Painvin, Gilles Perrot and Raphaël Couturier. *"Brick Orientation Adjustment in the Automotive Industry using Image Processing Techniques"*. In **2022 International Conference on Control, Decision and Information Technologies (CoDIT'22)**.

BIBLIOGRAPHY

- [1] WANG, J., CHEN, Q., AND CHEN, Y. **Rbf kernel based support vector machine with universal approximation and its application.** In *International symposium on neural networks* (2004), Springer, pp. 512–517.
- [2] KOTSIANTIS, S., KANELLOPOULOS, D., PINTELAS, P., AND OTHERS. **Handling imbalanced datasets: A review.** *GESTS International Transactions on Computer Science and Engineering* 30, 1 (2006), 25–36.
- [3] HARVEL, G., CHANG, J.-S., EWING, D., FANSON, P., AND KAKINOHANA, M. **Measurement of multi-dimension soot distribution in diesel particulate filters by a dynamic neutron radiography.** Tech. rep., SAE Technical Paper, 2009.
- [4] MENA, L., AND GONZALEZ, J. A. **Symbolic one-class learning from imbalanced datasets: application in medical diagnosis.** *International Journal on Artificial Intelligence Tools* 18, 02 (2009), 273–309.
- [5] GOODFELLOW, I. J., POUGET-ABADIE, J., MIRZA, M., XU, B., WARDE-FARLEY, D., OZAIR, S., COURVILLE, A., AND BENGIO, Y. **Generative adversarial networks.** *arXiv preprint arXiv:1406.2661* (2014).
- [6] CHEN, T., AND GUESTRIN, C. **Xgboost: A scalable tree boosting system.** *CoRR abs/1603.02754* (2016).
- [7] GOODFELLOW, I. **Nips 2016 tutorial: Generative adversarial networks.** *arXiv preprint arXiv:1701.00160* (2016).
- [8] REZENDE, E., RUPPERT, G., CARVALHO, T., RAMOS, F., AND DE GEUS, P. **Malicious software classification using transfer learning of resnet-50 deep neural network.** In *2017 16th IEEE International Conference on Machine Learning and Applications (ICMLA)* (2017), IEEE, pp. 1011–1014.
- [9] SAMEK, W., WIEGAND, T., AND MÜLLER, K.-R. **Explainable artificial intelligence: Understanding, visualizing and interpreting deep learning models.** *arXiv preprint arXiv:1708.08296* (2017).
- [10] SELVARAJU, R. R., COGSWELL, M., DAS, A., VEDANTAM, R., PARIKH, D., AND BATRA, D. **Grad-cam: Visual explanations from deep networks via gradient-based**

- localization.** In *Proceedings of the IEEE international conference on computer vision* (2017), pp. 618–626.
- [11] HOLCOMB, S. D., PORTER, W. K., AULT, S. V., MAO, G., AND WANG, J. **Overview on deepmind and its alphago zero ai.** In *Proceedings of the 2018 international conference on big data and education* (2018), pp. 67–71.
- [12] LIU, T., BAO, J., WANG, J., AND ZHANG, Y. **A hybrid cnn-lstm algorithm for online defect recognition of co2 welding.** *Sensors* 18, 12 (2018), 4369.
- [13] MIKOŁAJCZYK, A., AND GROCHOWSKI, M. **Data augmentation for improving deep learning in image classification problem.** In *2018 international interdisciplinary PhD workshop (IIPhDW)* (2018), IEEE, pp. 117–122.
- [14] OZA, P., AND PATEL, V. M. **One-class convolutional neural network.** *IEEE Signal Processing Letters* 26, 2 (2018), 277–281.
- [15] SANKUPELLAY, M., AND KONOVALOV, D. **Bird call recognition using deep convolutional neural network resnet-50.** In *Proc. ACOUSTICS* (2018), vol. 7, pp. 1–8.
- [16] BRINKER, T. J., HEKLER, A., ENK, A. H., KLODE, J., HAUSCHILD, A., BERKING, C., SCHILLING, B., HAFERKAMP, S., SCHADENDORF, D., HOLLAND-LETZ, T., AND OTHERS. **Deep learning outperformed 136 of 157 dermatologists in a head-to-head dermoscopic melanoma image classification task.** *European Journal of Cancer* 113 (2019), 47–54.
- [17] GONG, Z., ZHONG, P., YU, Y., HU, W., AND LI, S. **A cnn with multiscale convolution and diversified metric for hyperspectral image classification.** *IEEE Transactions on Geoscience and Remote Sensing* 57, 6 (2019), 3599–3618.
- [18] LONDON, A. J. **Artificial intelligence and black-box medical decisions: accuracy versus explainability.** *Hastings Center Report* 49, 1 (2019), 15–21.
- [19] WEN, L., LI, X., AND GAO, L. **A transfer convolutional neural network for fault diagnosis based on resnet-50.** *Neural Computing and Applications* (2019), 1–14.
- [20] AHAMMAD, S. H., RAJESH, V., RAHMAN, M. Z. U., AND LAY-EKUAKILLE, A. **A hybrid cnn-based segmentation and boosting classifier for real time sensor spinal cord injury data.** *IEEE Sensors Journal* 20, 17 (2020), 10092–10101.
- [21] AHLAWAT, S., AND CHOUDHARY, A. **Hybrid cnn-svm classifier for handwritten digit recognition.** *Procedia Computer Science* 167 (2020), 2554–2560.
- [22] AKIL, M., ELLOUMI, Y., AND KACHOURI, R. **Detection of retinal abnormalities in fundus image using cnn deep learning networks,** 2020.

- [23] ALSHEMALI, B., AND KALITA, J. **Improving the reliability of deep neural networks in nlp: A review.** *Knowledge-Based Systems 191* (2020), 105210.
- [24] CROSBY, J., CHEN, S., LI, F., MACMAHON, H., AND GIGER, M. **Network output visualization to uncover limitations of deep learning detection of pneumothorax.** In *Medical Imaging 2020: Image Perception, Observer Performance, and Technology Assessment* (2020), vol. 11316, International Society for Optics and Photonics, p. 113160O.
- [25] CRUZ, Y. J., RIVAS, M., QUIZA, R., BERUVIDES, G., AND HABER, R. E. **Computer vision system for welding inspection of liquefied petroleum gas pressure vessels based on combined digital image processing and deep learning techniques.** *Sensors 20*, 16 (2020), 4505.
- [26] GAO, Z., ZHANG, Y., AND LI, Y. **Extracting features from infrared images using convolutional neural networks and transfer learning.** *Infrared Physics & Technology 105* (2020), 103237.
- [27] GHOSE, S., SINGH, N., AND SINGH, P. **Image denoising using deep learning: Convolutional neural network.** In *2020 10th International Conference on Cloud Computing, Data Science & Engineering (Confluence)* (2020), IEEE, pp. 511–517.
- [28] GOUR, M., JAIN, S., AND SUNIL KUMAR, T. **Residual learning based cnn for breast cancer histopathological image classification.** *International Journal of Imaging Systems and Technology* (2020).
- [29] GUZUEVA, E., VEZIROV, T., BEYBALAEVA, D., BATUKAEV, A., AND CHAPLAEV, K. G. **The impact of automation of agriculture on the digital economy.** In *IOP Conference Series: Earth and Environmental Science* (2020), vol. 421, IOP Publishing, p. 022047.
- [30] HSIEH, T.-H., AND KIANG, J.-F. **Comparison of cnn algorithms on hyperspectral image classification in agricultural lands.** *Sensors 20*, 6 (2020), 1734.
- [31] JIANG, D., LI, F., YANG, Y., AND YU, S. **A tomato leaf diseases classification method based on deep learning.** In *2020 Chinese Control And Decision Conference (CCDC)* (2020), IEEE, pp. 1446–1450.
- [32] JIAQIANG, E., ZHENG, P., HAN, D., ZHAO, X., AND DENG, Y. **Effects analysis on soot combustion performance enhancement in a rotary diesel particulate filter unit during continuous microwave heating.** *Fuel 276* (2020), 118043.
- [33] LORENCIN, I., ANDELIĆ, N., ŠPANJOL, J., AND CAR, Z. **Using multi-layer perceptron with laplacian edge detector for bladder cancer diagnosis.** *Artificial Intelligence in Medicine 102* (2020), 101746.

- [34] MROZEK, P., PANNEERSELVAM, J., AND BAGDASAR, O. **Efficient resampling for fraud detection during anonymised credit card transactions with unbalanced datasets.** In *2020 IEEE/ACM 13th International Conference on Utility and Cloud Computing (UCC)* (2020), IEEE, pp. 426–433.
- [35] OCAÑA, M. I. G., ROMÁN, K. L.-L., URZELAI, N. L., BALLESTER, M. Á. G., AND OLIVER, I. M. **Medical image detection using deep learning.** In *Deep Learning in Healthcare*. Springer, 2020, pp. 3–16.
- [36] OSAWA, Y., WATANUKI, K., KAEDE, K., AND MURAMATSU, K. **Visualization of features in multivariate gait data: Use of a deep learning for the visualization of body parts and their timing during gait training.** In *International Conference on Applied Human Factors and Ergonomics* (2020), Springer, pp. 1007–1013.
- [37] PAN, H., PANG, Z., WANG, Y., WANG, Y., AND CHEN, L. **A new image recognition and classification method combining transfer learning algorithm and mobilenet model for welding defects.** *IEEE Access* 8 (2020), 119951–119960.
- [38] RADKE, A. M., DANG, M. T., AND TAN, A. **Using robotic process automation (rpa) to enhance item master data maintenance process.** *LogForum* 16, 1 (2020).
- [39] ROSSI, A., AHMED, N., SALEHIN, S., CHOUDHURY, T. H., AND SAROWAR, G. **Real-time lane detection and motion planning in raspberry pi and arduino for an autonomous vehicle prototype.** *arXiv preprint arXiv:2009.09391* (2020).
- [40] SALIM, R., MANDUCHI, A., AND JOHANSSON, A. **Investment decisions on automation of manufacturing in the wood products industry: A case study.** *Bio-Products Business* (2020), 1–12.
- [41] SHEVCHIK, S., LE-QUANG, T., MEYLAN, B., FARAHANI, F. V., OLBINADO, M. P., RACK, A., MASINELLI, G., LEINENBACH, C., AND WASMER, K. **Supervised deep learning for real-time quality monitoring of laser welding with x-ray radiographic guidance.** *Scientific reports* 10, 1 (2020), 1–12.
- [42] SULTANA, F., SUFIAN, A., AND DUTTA, P. **A review of object detection models based on convolutional neural network.** In *Intelligent Computing: Image Processing Based Applications*. Springer, 2020, pp. 1–16.
- [43] TAN, P.-Q., WANG, D.-Y., YAO, C.-J., ZHU, L., WANG, Y.-H., WANG, M.-H., HU, Z.-Y., AND LOU, D.-M. **Extended filtration model for diesel particulate filter based on diesel particulate matter morphology characteristics.** *Fuel* 277 (2020), 118150.
- [44] THECKEDATH, D., AND SEDAMKAR, R. **Detecting affect states using vgg16, resnet50 and se-resnet50 networks.** *SN Computer Science* 1, 2 (2020), 1–7.

- [45] TIAN, C., XU, Y., LI, Z., ZUO, W., FEI, L., AND LIU, H. **Attention-guided cnn for image denoising.** *Neural Networks* 124 (2020), 117–129.
- [46] TIAN, C., XU, Y., AND ZUO, W. **Image denoising using deep cnn with batch renormalization.** *Neural Networks* 121 (2020), 461–473.
- [47] WANG, B., HU, S. J., SUN, L., AND FREIHEIT, T. **Intelligent welding system technologies: State-of-the-art review and perspectives.** *Journal of Manufacturing Systems* 56 (2020), 373–391.
- [48] YANG, Y., PAN, L., MA, J., YANG, R., ZHU, Y., YANG, Y., AND ZHANG, L. **A high-performance deep learning algorithm for the automated optical inspection of laser welding.** *Applied Sciences* 10, 3 (2020), 933.
- [49] YU, C., HAN, R., SONG, M., LIU, C., AND CHANG, C.-I. **A simplified 2d-3d cnn architecture for hyperspectral image classification based on spatial-spectral fusion.** *IEEE Journal of Selected Topics in Applied Earth Observations and Remote Sensing* (2020).
- [50] ZHOU, F., YANG, S., FUJITA, H., CHEN, D., AND WEN, C. **Deep learning fault diagnosis method based on global optimization gan for unbalanced data.** *Knowledge-Based Systems* 187 (2020), 104837.
- [51] ABDULAAL, M. J., CASSON, A. J., AND GAYDECKI, P. **Critical analysis of cross-validation methods and their impact on neural networks performance inflation in electroencephalography analysis.** *IEEE Canadian Journal of Electrical and Computer Engineering* 44, 1 (2021), 75–82.
- [52] AGRAWAL, P., CHAUDHARY, D., MADAAN, V., ZABROVSKIY, A., PRODAN, R., KIMOVSKI, D., AND TIMMERER, C. **Automated bank cheque verification using image processing and deep learning methods.** *Multimedia Tools and Applications* 80, 4 (2021), 5319–5350.
- [53] CHEN, J., ZHANG, D., SUZAUDDOLA, M., NANEHKARAN, Y. A., AND SUN, Y. **Identification of plant disease images via a squeeze-and-excitation mobilenet model and twice transfer learning.** *IET Image Processing* 15, 5 (2021), 1115–1127.
- [54] DANDEKAR, N., KULKARNI, J., RAUT, R., AND RAUT, K. **Extracting features from the fundus image using canny edge detection method for predetection of diabetic retinopathy.** *VIVA-Tech International Journal for Research and Innovation* 1, 4 (2021), 1–6.
- [55] EL HACHEM, C., PERROT, G., PAINVIN, L., AND COUTURIER, R. **Automation of quality control in the automotive industry using deep learning algorithms.** In

- 2021 International Conference on Computer, Control and Robotics (ICCCR)* (2021), IEEE, pp. 123–127.
- [56] EL HACHEM, C., PERROT, G., PAINVIN, L., ERNST-DESMULIER, J.-B., AND COUTURIER, R. **Welding seam classification in the automotive industry using deep learning algorithms.** In *2021 IEEE International Conference on Industry 4.0, Artificial Intelligence, and Communications Technology (IAICT)* (2021), IEEE, pp. 235–240.
- [57] GOH, G., SING, S., AND YEONG, W. **A review on machine learning in 3d printing: Applications, potential, and challenges.** *Artificial Intelligence Review* 54, 1 (2021), 63–94.
- [58] HAQ, M. A., RAHAMAN, G., BARAL, P., AND GHOSH, A. **Deep learning based supervised image classification using uav images for forest areas classification.** *Journal of the Indian Society of Remote Sensing* 49, 3 (2021), 601–606.
- [59] JIA, S., JIANG, S., LIN, Z., LI, N., XU, M., AND YU, S. **A survey: Deep learning for hyperspectral image classification with few labeled samples.** *Neurocomputing* 448 (2021), 179–204.
- [60] KIM, Y., AND DODDIBA, G. **A novel method for simultaneous evaluation of particle geometry by using image processing analysis.** *Powder Technology* 393 (2021), 60–73.
- [61] KULKARNI, U., MEENA, S., GURLAHOSUR, S. V., AND BHOGAR, G. **Quantization friendly mobilenet (qf-mobilenet) architecture for vision based applications on embedded platforms.** *Neural Networks* 136 (2021), 28–39.
- [62] KUMAR, A., VASHISHTHA, G., GANDHI, C., ZHOU, Y., GLOWACZ, A., AND XIANG, J. **Novel convolutional neural network (ncnn) for the diagnosis of bearing defects in rotary machinery.** *IEEE Transactions on Instrumentation and Measurement* 70 (2021), 1–10.
- [63] KUMAR, P., AND SHANKAR HATI, A. **Convolutional neural network with batch normalisation for fault detection in squirrel cage induction motor.** *IET Electric Power Applications* 15, 1 (2021), 39–50.
- [64] LEE, J., AND PARK, K. **Gan-based imbalanced data intrusion detection system.** *Personal and Ubiquitous Computing* 25, 1 (2021), 121–128.
- [65] LIU, Y., ZHANG, Z., LIU, X., WANG, L., AND XIA, X. **Performance evaluation of a deep learning based wet coal image classification.** *Minerals Engineering* 171 (2021), 107126.

- [66] MANWAR, R., ZAFAR, M., AND XU, Q. **Signal and image processing in biomedical photoacoustic imaging: a review.** *Optics 2*, 1 (2021), 1–24.
- [67] MARCUS, J. **Challenges and frontiers in implementing artificial intelligence in process industry.** *Impact and Opportunities of Artificial Intelligence Techniques in the Steel Industry: Ongoing Applications, Perspectives and Future Trends 1338* (2021), 1.
- [68] NGUGI, L. C., ABELWAHAB, M., AND ABO-ZAHHAD, M. **Recent advances in image processing techniques for automated leaf pest and disease recognition—a review.** *Information processing in agriculture 8*, 1 (2021), 27–51.
- [69] OSKOOEI, A., CHAU, S. M., WEISS, J., SRIDHAR, A., MARTÍNEZ, M. R., AND MICHEL, B. **Destress: deep learning for unsupervised identification of mental stress in firefighters from heart-rate variability (hrv) data.** In *Explainable AI in Healthcare and Medicine*. Springer, 2021, pp. 93–105.
- [70] PANDEY, A., LIU, C., WANG, Y., AND SARAF, Y. **Dual application of speech enhancement for automatic speech recognition.** In *2021 IEEE Spoken Language Technology Workshop (SLT) (2021)*, IEEE, pp. 223–228.
- [71] RALPH, B., AND STOCKINGER, M. **Digitalization and digital transformation in metal forming: key technologies, challenges and current developments of industry 4.0 applications.** In *Proceedings of the XXXIX. Colloquium on Metal Forming (2021)*.
- [72] SADIK, R., ANWAR, S., AND REZA, M. L. **Autismnet: Recognition of autism spectrum disorder from facial expressions using mobilenet architecture.** *International Journal 10*, 1 (2021).
- [73] SARWINDA, D., PARADISA, R. H., BUSTAMAM, A., AND ANGGIA, P. **Deep learning in image classification using residual network (resnet) variants for detection of colorectal cancer.** *Procedia Computer Science 179* (2021), 423–431.
- [74] SOUMAYA, Z., TAOUFIQ, B. D., BENAYAD, N., YUNUS, K., AND ABDELKRIM, A. **The detection of parkinson disease using the genetic algorithm and svm classifier.** *Applied Acoustics 171* (2021), 107528.
- [75] STELAND, A., AND PIETERS, B. E. **Cross-validation and uncertainty determination for randomized neural networks with applications to mobile sensors.** *arXiv preprint arXiv:2101.01990* (2021).
- [76] YANG, J., AND LI, M. **Construction characteristics and quality control measures under high altitude and cold conditions.** In *IOP Conference Series: Earth and Environmental Science (2021)*, vol. 676, IOP Publishing, p. 012109.

- [77] ZARE, S., AND AYATI, M. **Simultaneous fault diagnosis of wind turbine using multichannel convolutional neural networks.** *ISA transactions 108* (2021), 230–239.
- [78] ZHANG, Y., HONG, D., McCLEMENT, D., OLADOSU, O., PRIDHAM, G., AND SLANEY, G. **Grad-cam helps interpret the deep learning models trained to classify multiple sclerosis types using clinical brain magnetic resonance imaging.** *Journal of Neuroscience Methods 353* (2021), 109098.
- [79] HACHEM, C. E. **brick dataset website:** https://zenodo.org/record/5948822#.YgphXd_MLIW.
- [80] DOCUMENTATION, O. **Opencv website:** https://docs.opencv.org/3.4/d9/db0/tutorial_hough_lines.html.
- [81] DOCUMENTATION, O. **Opencv website:** https://docs.opencv.org/3.4/da/d22/tutorial_py_canny.html.
- [82] DOOR THROUGH A WINDOW, A. **Adtw website:** www.adtwlearn.com.
- [83] LYNC, S. **skill lync website:** <https://skill-lync.com>.
- [84] MACHINE, T. **Technox machine website:** <https://www.technoxmachine.com/blog/mig-vs-tig-welding>.
- [85] OMDENA. <https://omdena.com/blog/heatmap-machine-learning/>.
- [86] PHOTO DOCUMENTATION, W. **Wistiti photo website:** <https://www.wistitiphoto.com/cours-photo/reglages-de-base-photo-numerique>.
- [87] QUANTINSTI. <https://blog.quantinsti.com/gini-index/>.
- [88] UNIVERSITY, A. **Antonine university website:** <https://ua.edu.lb/>.

LIST OF FIGURES

2.1	OK sensor boss on the left, NOK sensor boss (spatters inside) on the right	15
2.2	Different types of end forming applied in the manufacturing industry	15
3.1	Artificial intelligence vs. Machine learning vs. Deep learning	18
3.2	Confusion matrix of an AI model	21
3.3	Convolution phase: parameters	23
3.4	Convolution phase: Step 1	23
3.5	Convolution phase: intermediate steps	24
3.6	Convolution phase: step 9 (last step)	24
3.7	Activation functions applied in deep learning	25
3.8	Pooling phase	25
3.9	Neural network architecture	26
3.10	Skip connection and bottleneck in ResNet50 Architecture	28
4.1	Sub-assembly part to be checked. The three types of screws and their expected locations are displayed by the means of the black arrows.	34
4.2	Sample of each class in the trained model	36
5.1	Butt joint types	42
5.2	Tee joint types	43
5.3	Corner joint types	43
5.4	Lap joint example	43
5.5	Edge joint example	44
5.6	Types of welding technologies	45
5.7	Reference weld (OK) and five possible defects (NOK) for MIG/MAG welding	45
5.8	Effect of MIG wire feed speed on the welding tested by cutting and etching	46

5.9	Measurement of the weld length	46
5.10	Diagram representing the main function (MF1) of visual inspection and its related parameters	47
5.11	Sub-assembly part to be checked	48
5.12	The camera installation in a Faurecia plant	49
5.13	Images collected for each reference part	49
5.14	Representation of alpha and beta angles used in the torch angle parameter	50
5.15	Examples of data augmentation techniques applied on weld1	53
6.1	Decision-making approach for MobileNet architecture	59
6.2	Heatmap visualization of OK and NOK weld2 images.	60
6.3	Distribution of weld3 images per classes' scores	62
6.4	Correlating classes' scores with Red Color Ratio for weld3 images	63
6.5	Proposed decision-making approach: adding Grad-CAM heatmap and Red Color Ratio	64
7.1	Example of a ceramic monolith	68
7.2	Stuffing technique	68
7.3	Image processing methods applied on the ceramic monolith	71
7.4	Experimental environment: installation of the Basler camera	72
7.5	Gain: 0 on the left, 30 in the middle and 60 on the right	73
7.6	Exposure time: 0.12 on the left, 0.48 in the middle and 0.80 on the right	73
7.7	Possible aperture values	73
7.8	Results of Canny-Hough and Laplacian-Hough with linear regression	74
7.9	Repeatability test validated with Canny-Hough method	75
8.1	Network architecture	78
8.2	Loading/Unloading side of a turntable in a Faurecia plant	79
8.3	Cycle time of a turntable	79
8.4	Welding side of a turntable in a Faurecia plant	80
8.5	HMI development steps	82
8.6	mockup representing the HMI management of a reference part	82

8.7	activity diagram example representing the test-decision node	83
8.8	communication between actors in a sequence diagram (arrows represent- ing messages	84
8.9	Representation of class diagram's elements	85
8.10	Integrating deep learning and image processing at a hidden time in the cycle of a turntable	86
8.11	Steps of Innovation Program Management System (IPMS)	86

LIST OF TABLES

4.1	Accuracy comparison between human-being check and ResNet50	37
4.2	Cycle time's comparison between human-being check and ResNet50	38
5.1	Distribution of collected images for OK and NOK classes	51
5.2	Comparison between different data augmentation filters applied on four welding seams	54
5.3	Results of cross validation applied on weld4	55
6.1	Best results reached with data augmentation techniques on weld1, weld2, weld3 and weld4	59
6.2	Proposed decision making results when applied on weld2 and weld3	65

Title: Automation of Quality Control and Reduction of Non-Compliance using Machine Learning Techniques at Faurecia Clean Mobility

Keywords: Deep Learning, Visual Inspection, Quality Control, Component Presence Control, Welding Seam Inspection, Geometric Control, Industry4.0

Abstract:

english abstract

Titre : Automation of Quality Control and Reduction of Non-Compliance using Machine Learning Techniques at Faurecia Clean Mobility

Mots-clés : Deep Learning, Visual Inspection, Quality Control, Component Presence Control, Welding Seam Inspection, Geometric Control, Industry4.0

Résumé :

french abstract